MUTUAL COUPLING STUDY

George F. Farrell, Jr.

Prepared by

General Electric Company
Heavy Military Electronics Department
Court Street
Syracuse, New York

G.E. Purchase Order No. EH-40039

31 March 1967

Prepared for

Lincoln Laboratory
Lexington, Massachusetts

Lincoln Laboratory Order No. PO C-487

MUTUAL COUPLING STUDY

George F. Farrell, Jr.

Prepared by

General Electric Company
Heavy Military Electronics Department
Court Street
Syracuse, New York

G.E. Purchase Order No. EH-40039

31 March 1967

Prepared for

Lincoln Laboratory
Lexington, Massachusetts

PRIME CONTRACT AF 19(628)-5167

Lincoln Laboratory Order No. PO C-487

FOREWORD

An error affecting only the triangular grid was pointed out in the defining equations for the radiation admittance just shortly before publication of this report. That error has been corrected and the equations as they are given in the appendix are now correct. As a result, the numbers given in the body of the report for any quantity pertaining to the triangular grid are wrong and should not be used for any design purpose. The error is one of magnitude only and does not affect the validity of the comparison of mode amplitude with mode amplitude if the comparison is restricted to ordering the modes relative to one another. The numbers given for these quantities should not be compared with experiment. A valid comparison with experiment is given in the text (Figure 5) for the triangular grid and this was done with the corrected equations. The error did not in any way affect the rectangular grid.

TABLE OF CONTENTS

LIST OF ILLUSTRATIONS

LIST OF TABLES

ACKNOWLEDGMENT

The author wishes to thank Mr. Bliss Diamond of Lincoln Laboratories, Lexington, Mass. for his interest and efforts in checking over the derivation of the defining equations for the radiation admittance.

ABSTRACT

This report gives the complete derivation (in an appendix) of the radiation admittance of a rectangular waveguide acting as an element in an infinite phased array. The derived equations are capable of predicting the experimentally observed anomalous notch that has been found to exist in arrays composed of large waveguides. The defining equations demonstrate that it is the existence of nonpropagating higher order modes inside the element waveguides that determine the behavior of an infinite array.

It was the purpose of this study to determine what waveguide modes were important for a reasonably confident prediction of the radiation admittance of a rectangular waveguide in an array. It is shown that the number of modes needed for this is not excessively great, but that more are needed if it is desired to predict the position of an anomalous notch with any great degree of confidence.

MUTUAL COUPLING STUDY

SECTION I

INTRODUCTION

In recent years, a very considerable effort has been made by a number of workers to determine the effects on the radiation characteristics of a radiating element when it is placed in an array of other such elements. It has been found that the radiation impedance (or admittance) of an element in an array, in addition to having a variation with the scan angle of the array, exhibits a strong dependency upon the spacing between elements, the type of grid on which the element is placed, the size and shape of the element, and the proximity of the element to the edge of a finite array. It has been discovered that when an array becomes sufficiently large, a centrally located element does not have a measurably altered characteristic with further increase in the physical size of the array. For such a situation, one is free to consider the element as lying in an infinite array environment.

One of the first efforts to analyze an infinite array in terms of the field in the aperture of an element was that of Edelberg and Oliner (Ref. 1), who considered an infinite rectangular array of slots or rectangular waveguides. They assumed that the aperture field was in the TE_{10} mode only, without regard to element size or the angle to which the array was scanned. Experiments, however, indicated that if the waveguide element was sufficiently large, at least for the triangular grid, then a notch could appear in the element pattern at scan angles somewhat less than those corresponding to a visible grating lobe formation. Such a notch was not predicted by the grating lobe series approach, which was based upon the existence of only the TE_{10} mode in the waveguide aperture. Farrell and Kuhn (Ref. 2) have been able to predict the experimentally observed anomaly at least for the triangular grid array of waveguide horns by including in their analysis the possibility of higher order modes inside the elemental waveguide.

The purpose of this study was to determine which internal waveguide modes and how many external free space modes are necessary using Farrell and Kuhn's analysis (see Appendix) to adequately predict the behavior of a rectangular waveguide acting as an element in a phased array for any arbitrary scan angle of the array. Both rectangular and triangular grid geometries were to be considered, as well as the aspect ratio of the elemental horn. The purpose was to be accomplished by successively running the computer program developed by Farrell and Kuhn at each of several sine theta locations with varying

numbers of both internal (or waveguide) modes and external (or array-space) modes until the predicted admittance exhibited a sensibly stationary character with any increase in the number of modes. This numerical process was to be supplemented by analytical work when possible.

SECTION II

EXTERNAL MODE STUDY

This study program was begun with an already written but incompletely debugged computer program that had been written to solve for the radiation admittance of a waveguide in an array. The radiation admittance is given by (see Appendix)

$$Y = 2\left[\frac{\pi}{2}\right]^2 \frac{\frac{ab}{AB}}{\left[\frac{\gamma_{10}}{k_o}\right]} \left\{ J[(1, 1)\ (0, 0)] + j \sum_{p=1}^{\infty} {\sum_{q=0}^{\infty}}' p\, D_{pq}\, J[(p, 1)\ (q, 0)] \right.$$

$$\left. + j \sum_{p=0}^{\infty} \sum_{q=1}^{\infty} q\, C_{pq}\, K[(p, 1)\ (q, 0)] \right\} \tag{1}$$

where $J[(p, 1)\ (q, 0)]$ and $K[(p, 1)\ (q, 0)]$ are complex functions of the grid type, grid size, element size, array scan angle, and the waveguide mode eigennumbers p and q. The variables D_{pq} and C_{pq} are the waveguide higher order mode amplitude coefficients for the LSE mode type having the transverse component of electric field parallel (D_{pq}) with, and cross polarized (C_{pq}) with respect to, the incident TE_{10} mode. These coefficients are the solutions of the infinite family of complex simultaneous equations having the form

$$D_{pq}\left[\frac{\gamma_{PO}}{k_o}\right]^2 + F_{PQ} \sum_{p=1}^{\infty} {\sum_{q=0}^{\infty}}' p\, D_{pq}\, J[(p, P)\ (q, Q)]$$

$$+ PQ\, \frac{\lambda^2}{4ab}\, C_{PQ} + F_{PQ} \sum_{p=0}^{\infty} \sum_{q=0}^{\infty} q\, C_{pq}\, K[(p, P)\ (q, Q)] = j\, F_{PQ}\, J[(1, P)\ (0, Q)] \tag{2a}$$

and

$$PQ\, \frac{\lambda^2}{4ab}\, D_{PQ} + G_{PQ} \sum_{p=1}^{\infty} \sum_{q=0}^{\infty} p\, D_{pq}\, K[(p, P)\ (q, Q)]$$

$$+ \left[\frac{\gamma_{OQ}}{k_o}\right]^2 C_{PQ} + G_{PQ} \sum_{p=0}^{\infty} \sum_{q=1}^{\infty} q\, C_{pq}\, L[(p, P)\ (q, Q)] = j\, G_{PQ}\, K[(1, P)\ (0, Q)] \tag{2b}$$

where F_{PQ} and G_{PQ} are simple functions of the waveguide dimensions and the mode numbers and where $L[(p, P)\ (q, Q)]$ is a complex function of the same type as $J((*))$ and $K((*))$

above. The manner in which the waveguide modes have been defined allows us to designate a mode as being of dominant polarization (MD) or of cross polarization (MC). In a waveguide that is 0.6λ wide and 0.2667λ high, the modes are ordered by propagation constant as shown in Table 1. It will turn out, however, that the final waveguide mode order will depend upon the scan position in sine theta space rather than directly upon the waveguide propagation constant.

The complex functions J((*)), K((*)), and L((*)) have very similar forms, so that the study of the convergence properties of any one of them is adequate for all three. The simplest of the three was the one chosen for investigation. It is

$$K[(p, P)(q, Q)] = \frac{4}{ab\,k_o^2} \sum_{m=-\infty}^{\infty} \sum_{n=-\infty}^{\infty} \frac{\delta_{mn}^2}{1+I} \frac{\left[\frac{\beta_m a}{2}\right]^2 \left[\frac{\beta_n b}{2}\right]^2}{\left[\frac{\Gamma_{mn}}{k_o}\right]} \cdot S_m(p)\, S_m(P)\, S_n(q)\, S_n(Q) \tag{3}$$

where

$$\left[\frac{\Gamma_{mn}}{k_o}\right] = \sqrt{\left[\frac{\beta_m}{k_o}\right]^2 + \left[\frac{\beta_n}{k_o}\right]^2 - 1}$$

$$S_m(p) = \frac{\sin\left[\frac{\beta_m a}{2} - \frac{p\pi}{2}\right]}{\left[\frac{\beta_m a}{2}\right]^2 - \left[\frac{p\pi}{2}\right]^2}$$

$$\frac{\beta_m}{k_o} = X + \frac{m\lambda}{A}$$

$$\frac{\beta_n}{k_o} = Y + \frac{n\lambda}{B}$$

δ_{mn} - designate grid type

$X = \sin\Theta\cos\phi$

$Y = \sin\Theta\sin\phi$

TABLE 1

ORDER OF THE WAVEGUIDE LSE MODES BY PROPAGATION CONSTANT

p	q	Dominant MD_i i =	Cross MC_i i =	Propagation Constant $\frac{\gamma_{pq}}{k_o}$
1	0	0	--	j0.5527
2	0	1	--	1.3333
0	1	--	1	1.5860
1	1	2	2	1.7916
3	0	3	--	2.2913
2	1	4	3	2.3007
3	1	5	4	2.9606
4	0	6	--	3.1797
0	2	--	5	3.6141
4	1	7	6	3.6914
1	2	8	7	3.7089
2	2	9	8	3.9799
5	0	10	--	4.0448
3	2	11	9	4.3945
5	1	12	10	4.4583
4	2	13	11	4.9166
5	2	14	12	5.5157
0	3	--	13	5.5353
1	3	15	14	5.5977
2	3	16	15	5.7807
3	3	17	16	6.0737
4	3	18	17	6.4614
0	4	--	18	7.4329
1	4	19	19	7.4795
2	4	20	20	7.6175

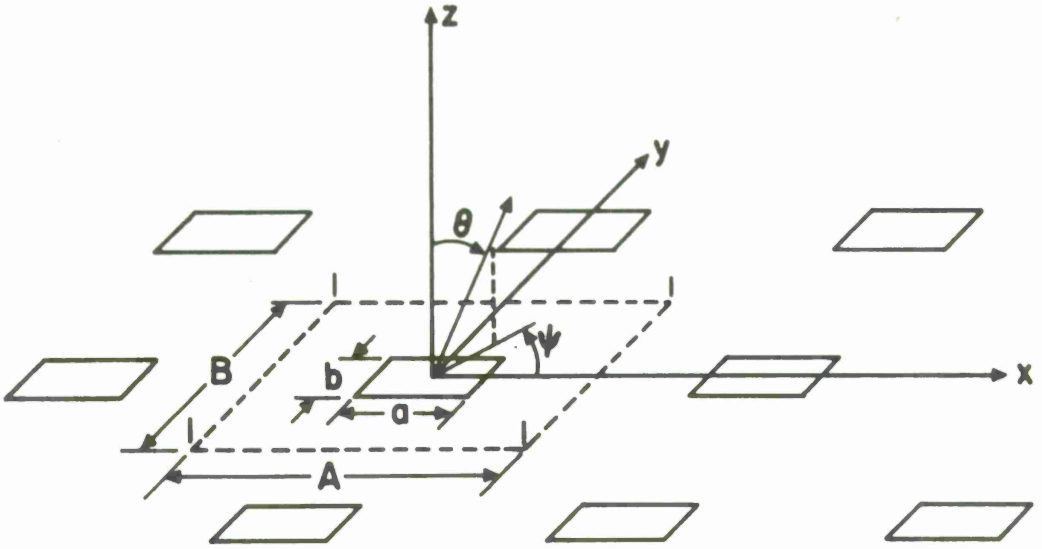

a. Rectangular Grid

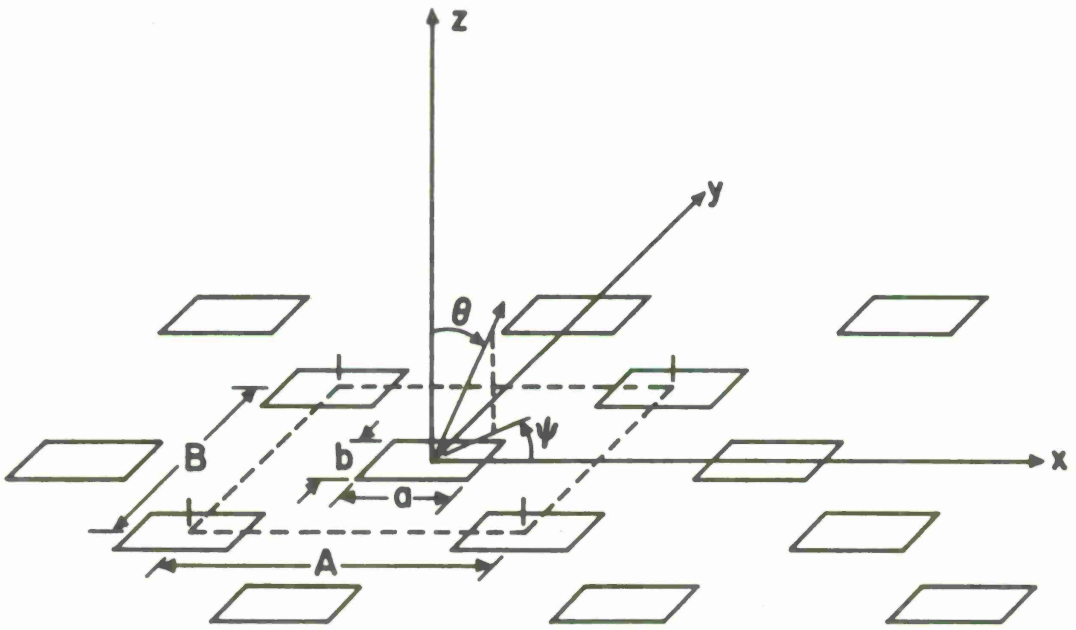

b. Triangular Grid

Figure 1. Array Geometry

In this equation the index numbers "m" and "n" are in actuality the eigennumbers of the higher order modes in the free space region of the array. Let us rewrite Equation (3) as

$$K[(p, P)(q, Q)] = \frac{4}{ab\, k_o^2} \sum_{n=-\infty}^{\infty} \left[\frac{\beta_n b}{2}\right]^2 S_n(q)\, S_n(Q)\, H_n(p, P) \tag{4}$$

where

$$H_n(p, P) = \sum_{m=-\infty}^{\infty} \frac{\delta_{mn}^2}{1+I} \frac{\left[\frac{\beta_m a}{2}\right]^2}{\left[\frac{\Gamma_{mn}}{k_o}\right]} S_m(p)\, S_m(P) \tag{5}$$

From purely physical considerations

$$0 \leq X \leq 1$$

$$\frac{a}{\lambda} \leq 1$$

so $0 \leq X \frac{a}{\lambda} \leq 1$. Further $A \geq a$, since "A" is the cell width while "a" is the width of the waveguide, so $\frac{a}{A} \leq 1$ (see Figure 1 for the grid geometries). As a result it is always possible to select a value of $|m| = M$ sufficiently large that

$$\frac{M\pi a}{A} >> \frac{X\pi a}{\lambda}$$

and consequently $\left[\frac{\beta_m a}{2}\right]$ approaches the value $\left[\frac{m\pi a}{A}\right]$ as "m" becomes large. We can select a still larger value of $|m| = M$ such that

$$\left|\frac{\beta_M a}{2}\right| >> \frac{p\pi}{2}$$

and

$$\left|\frac{\beta_M a}{2}\right| >> \frac{P\pi}{2}$$

Therefore we may write

$$H_n(p, P) = \sum_{m=-\infty}^{\infty} k_{mn}(p, P)$$

$$= \sum_{m=-\infty}^{-M} k_{mn}(p, P) + \sum_{m=-M}^{M} k_{mn}(p, P) + \sum_{m=M}^{\infty} k_{mn}(p, P)$$

$$\doteq \sum_{m=-M}^{M} k_{mn}(p, P) \qquad (6)$$

$$- \left[\frac{A}{\pi a}\right]^2 \sum_{m=M}^{\infty} \frac{\delta_{mn}^{\ 2}}{1+I} \frac{\cos \frac{2m\pi a}{A} \cos \left[\frac{2\pi Xa}{\lambda} - \frac{(p+P)\pi}{2}\right] - \cos \frac{(p-P)\pi}{2}}{m^2 \sqrt{\left[\frac{m\lambda}{A}\right]^2 + \left[\frac{\beta_n}{k_o}\right]^2 - 1}}$$

Consequently

$$H_n(p, P) \approx \sum_{m=-M}^{M} k_{mn}(p, P)$$

provided only that

$$M >> \frac{pA}{2a}$$

$$M >> \frac{PA}{2a}$$

since the sum on "m" from M to ∞ decreases at least as fast as $1/M^3$. For the summation on "n" we have from pure physical considerations

$$0 \leq Y \leq 1$$

$$\frac{b}{\lambda} \leq 1$$

so $0 \leq Y \frac{b}{\lambda} \leq 1$. Further $B \geq b$, since "B" is the height of the cell whereas "b" is the height of the encompassed waveguide, so $\frac{b}{B} \leq 1$. As a result it is always possible to select a value of $|n| = N$ sufficiently large that

$$\frac{N\pi b}{B} >> \frac{Y\pi b}{\lambda}$$

and consequently $\left[\frac{\beta_N b}{2}\right]$ approaches the value $\left[\frac{n\pi b}{B}\right]$ as "n" becomes large. We can select a still larger value of $|n| = N$ such that

$$\left|\frac{\beta_N b}{2}\right| \gg \frac{q\pi}{2}$$

and

$$\left|\frac{\beta_N b}{2}\right| \gg \frac{Q\pi}{2}$$

Therefore we may write

$$K[(p, P)(q, Q)] = \frac{4}{k_o^2 ab} \sum_{n=-\infty}^{\infty} \left[\frac{\beta_n b}{2}\right]^2 S_n(q)\, S_n(Q)\, H_n(p, P)$$

$$= \frac{4}{k_o^2 ab} \sum_{n=-\infty}^{\infty} k_n[(p, P)(q, Q)]$$

$$= \frac{4}{k_o^2 ab} \left\{ \sum_{n=-\infty}^{-N} k_n[(p, P)(q, Q)] + \sum_{n=-N}^{N} k_n[(p, P)(q, Q] \right.$$

$$\left. + \sum_{n=N}^{\infty} k_n[(p, P)(q, Q)] \right\} \tag{7}$$

$$\doteq \frac{4}{k_o^2 ab} \left\{ \sum_{n=-N}^{N} k_n[(p, P)(q, Q)] \right.$$

$$- \left[\frac{B}{\pi b}\right]^2 \sum_{n=N}^{\infty} \frac{H_n(p, P)}{n^2} \left[\cos \frac{2n\pi b}{B} \cos\left[\frac{2\pi Y b}{\lambda} - \frac{(q+Q)\pi}{2}\right]\right.$$

$$\left. \left. - \cos \frac{(q-Q)\pi}{2}\right]\right\}$$

$$\approx \frac{4}{k_o^2 ab} \sum_{n=-N}^{N} k_n[(p, P)(q, Q)]$$

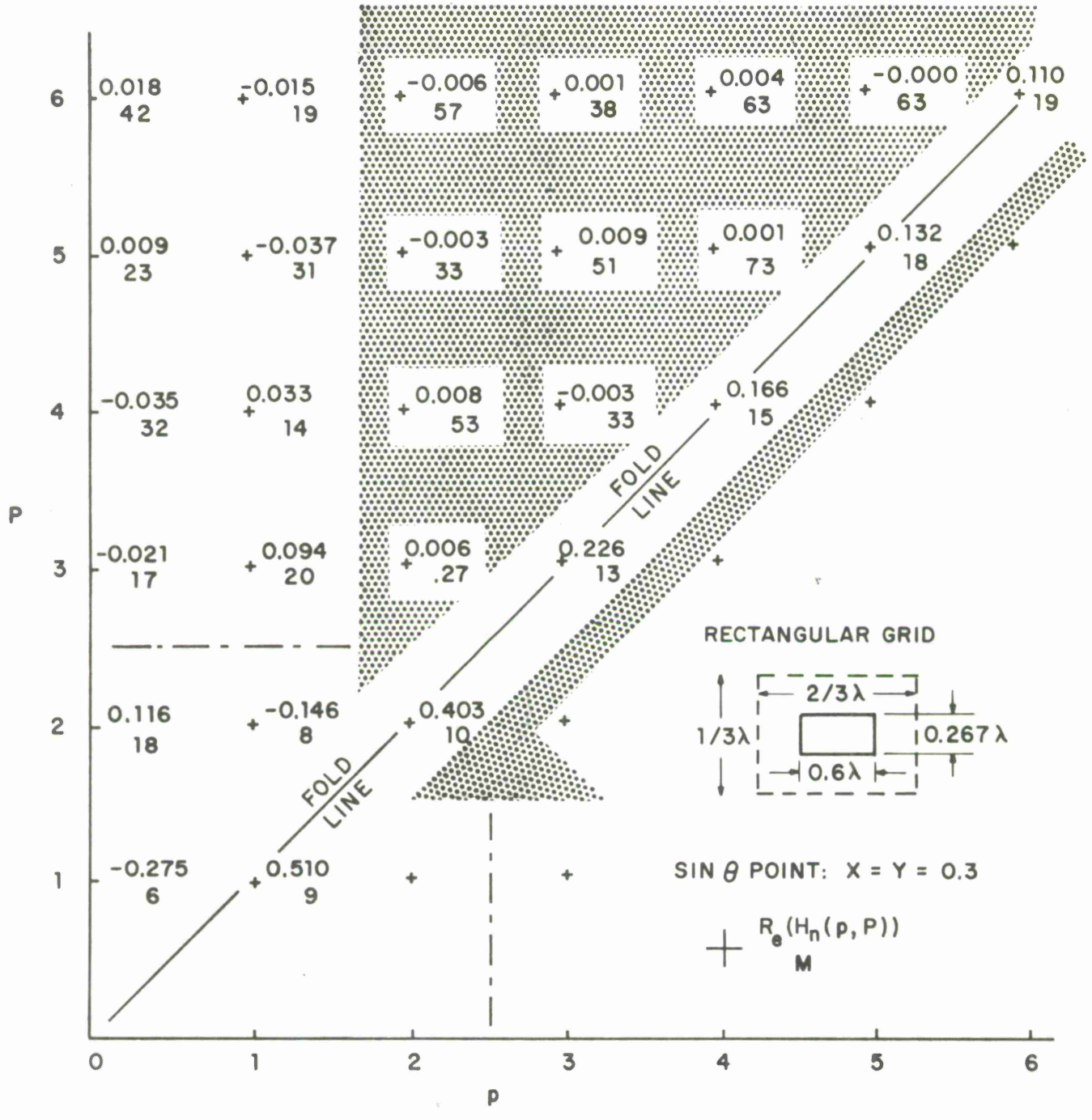

Figure 2. A Map of the Real Part of $H_n(p, P)$ and the Number of Iterations (M) Necessary for Convergence as a Function of p and P

provided only that

$$M >> \frac{pA}{2a}, \quad M >> \frac{PA}{2a}$$

$$N >> \frac{qB}{2b}, \quad N >> \frac{QB}{2b}$$

since the sum on "n" from N to ∞ decreases at least as fast as $1/N^3$.

Equation (5) was programmed for computer solution and data was obtained for n = 0, with a range for p and P from 0 to 7. The value of the sum was printed out for each value of $\pm$ m to a maximum absolute value of M = 80, at each of 10 points in sine theta space. For the purpose of evaluating the resulting mass of data, it was assumed that the accumulated value of the sum at |m| = 80 was the true value of the sum and that the sum had converged at some smaller value of |m| if the attained value were within 0.01 percent of the final value. Figure 2 is a map of the final value of the sum of Equation (5) and the value of "M" at which it was assumed to have converged. Figure 2 is for a representative point in sine theta space (X = 0.3 = Y) for a rectangular grid having $\frac{A}{\lambda} = 0.667$, $\frac{B}{\lambda} = 0.3333$, and rectangular waveguides having $\frac{a}{\lambda} = 0.6$ and $\frac{b}{\lambda} = 0.2667$. Table 2 is a sample case for which p = 1, P = 3. The conclusion that was drawn from the mass of data in general and which is borne out by Figure 2 is that the maximum values for $H_n(p, P)$ occur when p = P, and are attained with relatively few terms. Large values for $H_n(p, P)$ are obtained with only a few terms when both p and P are 2 or less and if $p \neq P$. Smaller values are obtained within a reasonable number of terms if p (or P) is zero or unity, when P (or p) is 3 or greater. Insignificant values for the sum $H_n(p, P)$ occur everywhere else but each requires a very large number of terms. In the unshaded region it is easily seen that M need not exceed 32 for all values of P less than or equal to 5.

TABLE 2

$$H_n(p, P) = \sum_{m=-M}^{M} k_{mn}(p, P) \text{ for } n = 0$$

M	$R_e\{H_o(p, P)\}$	$I_m\{H_o(p, P)\}$
0	0.	0.005359
1	0.136202	0.005359
2	0.099736	0.005359
3	0.096535	0.005359
4	0.095597	0.005359
5	0.095152	0.005359
6	0.094847	0.005359
7	0.094600	0.005359
8	0.094393	0.005359
9	0.094228	0.005359
10	0.094105	0.005359
11	0.094020	0.005359
12	0.093966	0.005359
13	0.093934	0.005359
14	0.093915	0.005359
15	0.093900	0.005359
16	0.093886	0.005359
17	0.093871	0.005359
18	0.093854	0.005359
19	0.093837	0.005359
20	0.093822	0.005359
21	0.093810	0.005359
22	0.093801	0.005359
23	0.093796	0.005359
24	0.093792	0.005359
-	-	-
-	-	-
-	-	-
79	0.093730	0.005359
80	0.093730	0.005359

SECTION III

STUDY OF THE MATRIX

Equation (3) exhibits a symmetry of form in m, p, P versus n, q, Q so that a function $H_m(q, Q)$ could have been considered instead of the $H_n(p, P)$ given by Equation (5), and the general results expressed above would have been essentially the same. Therefore, we may expect the major values for $K[(p, P)(q, Q)]$ of Equation (3) to occur when $p = P$ and $q = Q$, also when p, P, q, Q are all small (say ≤ 2), and also when p (or P) and q (or Q) are either zero or unity for larger values of P (or p) and Q (or q), say greater than 2. For all other values of p, P, q, Q we may expect the value of $K[(p, P)(q, Q)]$ to become almost vanishingly small. If it is assumed that these other values of p, P, q, Q yield such small values that they may justifiably be assumed to be identically zero, then the matrix for the left-hand side of Equations (2) will look like what is shown in Figure 3 where the 0's and 1's denote "blank" and "filled" matrix elements, respectively. Figure 3 was computed for 19 dominant (MD = 19) and 20 cross (MC = 20) modes inside the waveguide aperture. On this basis, of the 1521 possible elements only 533 need to be calculated. If it is assumed that all elements are equally laborious to calculate, even if the value is vanishingly small, then there is a 65 percent reduction in both time and labor in computing the matrix by retaining only the indicated elements and by setting the other elements to zero.

Table 3 is a portion of the matrix for the left-hand side of Equations (2) where the upper left quadrant is for the D_{PQ} part of Equation (2a), the upper right is for the C_{PQ} part of Equation (2a), the lower left quadrant is for the D_{PQ} part of Equation (2b), and the lower left is for the C_{PQ} part of Equation (2b). The portion of the matrix given was computed with M equal to 30 for the same grid as is shown in Figure 2 and at the sine theta point $X = 0.4 = Y$. The magnitude of the elements of the matrix bears out the expectation that the major values should occur when $p = P$ and $q = Q$. Most of the other values that are given are very small except when p, P, q, Q are all small, for which case the elements are slightly larger, as is also the case when p (or P) and q (or Q) are either zero or unity. This is also in keeping with the expectation mentioned above.

There are some very interesting characteristics that show up in the matrix. Table 4 is a list of the approximate absolute value of the elements along the main diagonal and along the two subdiagonals of the matrix a part of which is shown in Table 3. Inspection of the table will show that for the "dominant" modes there is a more or less constant value for the main diagonal matrix element associated with a particular value of "p," regardless of the value

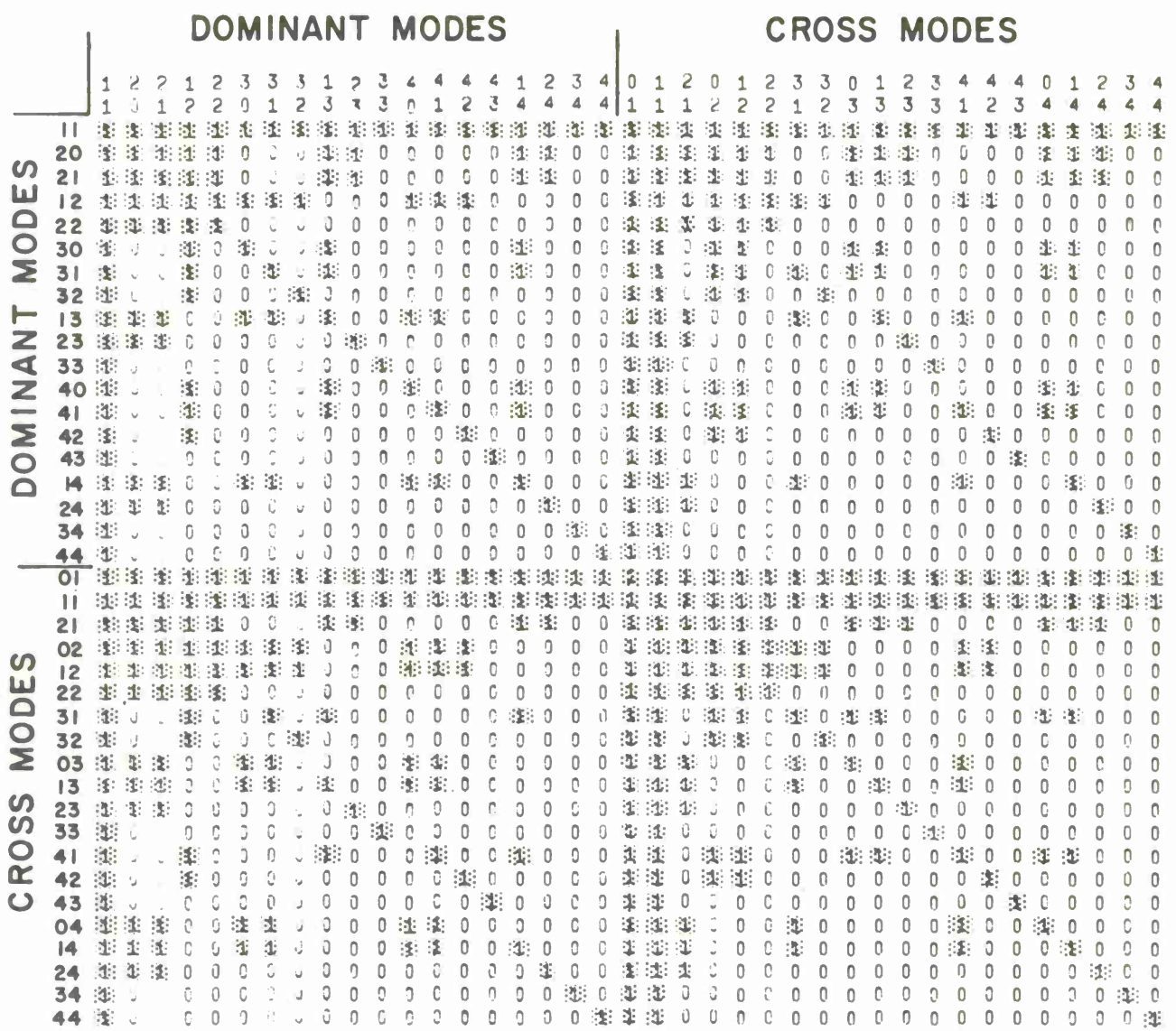

Figure 3. The Filling of the "Empty Matrix"

TABLE 3

ABSOLUTE VALUES OF THE ELEMENTS IN PART OF THE MATRIX

PQ \ pq	11	20	21	12	22	01	11	21	02	12	22		10
11	0.51	0.1	0.02	0.02	0.005	0.06	2.41	0.047	0.023	0.078	0.005		0.29
20	0.04	2.89	0.06	0.004	0.059	0.11	0.15	0.15	0.06	0.036	0.24		0.26
21	0.027	0.02	2.78	0.006	0.031	0.29	0.12	5.06	0.05	0.011	0.14		0.12
12	0.04	0.02	0.011	0.65	0.022	0.025	0.08	0.005	0.06	5.72	0.05		0.12
22	0.01	0.35	0.054	0.023	3.16	0.047	0.01	0.12	0.56	0.10	11.4		0.02
01	0.025	0.11	0.11	0.005	0.01	3.75	0.43	0.06	0.23	0.057	0.038		0.246
11	2.41	0.39	0.1	0.039	0.004	0.95	3.07	0.29	0.13	0.28	0.07		0.372
21	0.06	0.53	5.06	0.003	0.07	0.19	0.38	3.42	0.11	0.12	0.23		0.252
02	0.024	0.17	0.043	0.027	0.25	0.51	0.13	0.09	24.3	0.13	0.50		0.079
12	0.16	0.20	0.019	5.72	0.09	0.29	0.57	0.15	0.26	23.7	0.16		0.839
22	0.013	1.45	0.24	0.048	11.43	0.19	0.16	0.40	1.11	0.17	23.7		0.107

TABLE 4

APPROXIMATE MAIN AND SUBDIAGONAL MATRIX ELEMENT VALUES

PQ	Main Diagonal		Both Subdiagonals
	Dominant	Cross	
01	--	3.75	--
11	0.51	3.07	2.41
20	2.89	--	--
21	2.78	3.42	5.06
02	--	24.26	--
12	0.65	23.66	5.72
22	3.16	23.66	11.43
30	9.39	--	--
31	8.78	3.9	7.91
32	9.56	23.78	17.21
03	--	57.73	--
13	0.63	56.66	8.74
23	3.26	56.76	17.47
33	9.75	56.96	26.25
40	18.56	--	--
41	17.55	4.14	10.90
42	18.54	23.89	23.02
43	18.86	57.13	35.07
04	--	106.5	--
14	0.63	105.2	11.93
24	3.35	105.2	23.84
34	9.97	105.2	35.75
44	19.23	105.2	47.66

for "q." For the "cross" modes, however, the more or less constant value for the main diagonal element is associated with a particular value of "q" regardless of the value of "p." This fact is shown in Table 5.

TABLE 5

CONSTANCY OF MAIN DIAGONAL ELEMENT WITH p OR q

p or q	1	2	3	4
"dominant" (p) value	0.6	3.0	9.5	18.5
$\left[\frac{\gamma_{PO}}{k_o}\right]^2$	0.305	1.78	5.25	10.1
"cross" (q) value	3.8	24.0	57.0	105.0
$\left[\frac{\gamma_{OP}}{k_o}\right]^2$	2.51	13.05	30.6	55.2

For the subdiagonal elements, however, it is the product of "p" and "q" that appears to set a more or less constant value of an element so that

p*q	1	2	3	4	6	8	9	12	16
element value	2.4	5.5	8.0	11.0	17.3	23.5	26.2	35.5	47.7
$\left[PQ\ \frac{\lambda^2}{4ab}\right]$	1.56	3.12	4.68	6.25	9.36	12.5	14.05	18.75	25.0

Referring to Equation (2a), it can be seen that in the upper portion of the matrix the main diagonal elements are augmented by $\left[\frac{\gamma_{PO}}{k_o}\right]^2$, which is a quantity that is independent of "Q" (or "q"). This tends to explain the finding that there is more or less constant value for the main diagonal dominant mode elements associated with a value for "p" independent of "q." Also, in the upper portion of the matrix we can see that the subdiagonal elements are augmented by $\left[\frac{\lambda^2}{4ab}\ PQ\right]$, a quantity varying as the product of p and q.

In the lower portion of the matrix we refer to Equation (2b) from which we see that the subdiagonal elements are augmented by $\left[\frac{\lambda^2}{4ab}\ PQ\right]$ and the main diagonal elements by

TABLE 6

COMPARISON OF A FULL MATRIX WITH AN EMPTY MATRIX FOR A RECTANGULAR GRID ARRAY

$\frac{A}{\lambda} = 0.6666$, $\frac{B}{\lambda} = 0.3333$, $\frac{a}{\lambda} = 0.6000$, $\frac{b}{\lambda} = 0.2666$

AT SINE THETA SPACE POINT

X = 0.500, Y = 0.750

P	Q	Full Matrix		Empty Matrix	
		G	B	G	B
Dominant Mode Contribution					
1	0	1.350472	0.012931	1.350472	0.012931
Principal Polarization Contribution					
1	1	-0.398926	0.142121	-0.392068	0.132788
2	0	-0.021533	0.016890	-0.023566	0.016588
2	1	-0.588906	0.354161	-0.577752	0.344447
1	2	-0.039054	-0.013363	-0.036654	-0.011529
2	2	0.006181	-0.001933	0.003594	-0.001816
3	0	0.006367	0.003354	0.007999	-0.005562
3	1	0.007268	-0.001699	-0.004212	-0.008395
3	2	0.000152	0.000182	0.000187	-0.000224
1	3	-0.032859	0.005586	-0.031-12	0.005581
2	3	-0.076873	0.039342	-0.077453	0.038602
3	3	0.002627	0.000462	0.000232	-0.003091
Cross-Polarization Contributions					
0	1	-0.065360	0.090943	-0.068132	0.090361
1	1	0.035677	0.020559	0.035948	0.022415
2	1	-0.070353	0.266874	-0.069723	0.260815
0	2	0.000266	0.001105	-0.000260	0.000816
1	2	0.000852	0.004222	0.000353	0.004340
2	2	0.000462	-0.002700	-0.000049	-0.001513
3	1	0.002122	-0.004717	-0.003549	-0.001461
3	2	0.000033	-0.000103	-0.000195	0.000073
0	3	-0.002189	0.002859	-0.000920	0.001242
1	3	0.003863	0.004180	0.003610	0.004183
2	3	-0.008335	0.038746	-0.008757	0.038766
3	3	0.000558	-0.001825	-0.002111	-0.000378
Total		0.112513	0.982060	0.105982	0.939979

$\left[\frac{\gamma_{OQ}}{k_o}\right]^2$. The augmentation of the subdiagonal elements is obviously again a product of p and q. The augmentation of the main diagonal elements in the lower portion of the matrix is by a quantity which varies with "q" and not with "p," and tends to explain the finding that these elements appear to have a more or less constant value associated with a value of "q" independent of the value of "p."

In both the upper and lower half of the matrix it can be seen that as "p" or "q" become large, both the main diagonal as well as the subdiagonal elements tend to become quite large. At the same time the element on the right-hand side of the equation tends to become small. As a result, one can see that the amplitude coefficient for a mode having "p" or "q" large can be expected to become relatively small. Therefore, it is reasonable to suppose that the number of modes necessary to yield an adequately accurate answer should not be excessively great.

The matrix emptying shown in Figure 3 was incorporated into the source program for the main problem and tested. Then a sample case for a distant intercardinal point in sine theta space was computed with both a filled matrix and an empty matrix for the simultaneous equations of Equations (2). The result (by mode contribution) is shown in Table 6 for a rectangular grid having $\frac{A}{\lambda} = 0.6666$, $\frac{B}{\lambda} = 0.3333$, and waveguide dimensions $\frac{a}{\lambda} = 0.6000$, $\frac{b}{\lambda} = 0.2666$, and assuming M = 25, at a sine theta position X = 0.5, Y = 0.75. Table 7 shows the overall result at four other points in sine theta space. It must be pointed out that the values for mode contributions and the totals for the conductance and susceptance as given in Tables 6 and 7 are incorrect because there was an error in the computer program by which they were computed. That error, however, does not invalidate the comparison of the two conditions of the same matrix since the error effects both conditions equally. It can be seen from the two tables that (as expected) the empty matrix predicts an answer of very reasonable accuracy as compared with the answer given by the full matrix. Comparison of the modes used as shown in Table 6 with the form of the emptied matrix of Figure 3 shows that the empty matrix solution is accomplished with about 57 percent of the time and labor that was necessary for the full matrix solution. The emptied matrix method of solving the simultaneous equations, however, is not without pitfalls because it is possible for it to predict a negative conductance in the near vicinity of an anomalous notch. This of course is physically impossible, but it does indicate the very close proximity of a notch and one could either accept it as being the notch, or rerun the region of the anomaly with a full matrix.

TABLE 7

COMPARISON OF FULL AND EMPTY MATRIX AT FOUR POINTS IN SINE THETA SPACE FOR A RECTANGULAR GRID ARRAY

$\frac{A}{\lambda} = 0.6666$, $\frac{B}{\lambda} = 0.3333$, $\frac{a}{\lambda} = 0.6000$, $\frac{b}{\lambda} = 0.2666$

		Empty Matrix		Full Matrix	
X	Y	G	B	G	B
0.100	0.100	1.062749	-0.427803	1.062851	-0.428704
0.	0.500	1.170263	-0.277261	1.181389	-0.277087
0.400	0.	0.873127	-0.313060	0.873079	-0.294184
0.400	0.400	1.154778	1.673230	1.280810	1.669984

As a case in point, Table 8 gives the radiation conductance and susceptance along an E-plane cut on a square grid array $\left[\frac{A}{\lambda} = \frac{B}{\lambda} = 0.6439\right]$ made up of square waveguides $\left[\frac{a}{\lambda} = \frac{b}{\lambda} = 0.5898\right]$ assuming the external mode range to be M = 25 and with MD = 4, MC = 4. As has been mentioned earlier, MD and MC refer to principal polarization and cross-polarization, respectively, of the LSE higher order modes inside the waveguides. These internal modes have been selected to be those having the greatest effect on the final answer in E-plane for the rectangular grid, of which the square grid is a special case. The matter of the selection of the modes and their number will be dealt with later in this report. The point of interest is at Y = H-plane sin $\Theta = 0.550$ under the "Empty Matrix" which has a negative conductance of G = -0.105573. That same point under the "Full Matrix" has a conductance G = 0.947626. Note, however, that a Y = 0.540 under the "Full Matrix" the conductance is G = 0.087137. That this point is an anomaly can be seen by referring to Table 9, which compares the "Full Matrix" advanced theory with the simple grating lobe series. According to the simple grating lobe series, the conductance is nearly a constant as the grating lobe onset position (Y = 0.553) is approached, but the susceptance is approaching infinity. At the grating lobe onset position the grating lobe series will predict a reflection coefficient of unity due to an infinite susceptance. The advanced theory, however, indicates a rapidly decreasing conductance which approaches (or becomes) zero at Y = 0.540. At this same point the susceptance is large so that there is a unity (or nearly unity) reflection coefficient due to the zero (or nearly zero) value of conductance. This is an anomaly because it is occurring at Y $\doteq$ 0.540, whereas the grating lobe onset null is at Y = 0.553.

TABLE 8

FULL AND EMPTY MATRIX SOLUTIONS FOR THE RADIATION ADMITTANCE ALONG AN E-PLANE CUT ON A SQUARE GRID ARRAY OF SQUARE WAVEGUIDES

"Empty Matrix"			"Full Matrix"		
Y	G	B	Y	G	B
0.400	0.886374	-0.045881	0.520	0.395083	1.153299
0.425	0.828882	0.057068	0.530	0.271361	1.608455
0.450	0.760308	0.191632	0.540	0.087137	2.584137
0.475	0.673096	0.381052	0.550	0.947626	8.063701
0.500	0.549421	0.684035	0.560	4.032689	0.302194
0.525	0.334051	1.315519	0.570	3.115006	0.199048
0.550	-0.105573	2.940993			
0.575	3.062249	-0.040632			
0.600	2.470087	-0.057913			
0.625	2.242991	-0.085334			
0.650	2.121039	-0.103686			

Y = E-plane sin θ

G = Radiation conductance

B = Radiation susceptance

SECTION IV

STUDY OF THE INTERNAL MODES

In all of the foregoing discussion no mention has been made concerning what waveguide modes are necessary to adequately define the final admittance value. With an infinite number of simultaneous equations to select from for the solution for the mode amplitude coefficients (D_{pq} and C_{pq}) as expressed by Equations (2a) and (2b), the first problem is to include enough of the higher order modes nearest cutoff in order that the solution of the truncated set will give values that converge to very nearly the right answer. Prior knowledge of the values for the coefficients or even their order of importance is completely unavailable. Unfortunately, the form of the expressions encountered in Equations (2a) and (2b) does not lend itself to analytically determining which modes are important or how many are needed for an adequate answer.

At one point in the program it was decided to see if the equations -- (2a) and (2b) -- should be reconstituted in terms of the TE and TM modes instead of the LSE modes. The mode coefficients are related as follows.

$$D_{pq} = K\left[E_{pq}\frac{p\pi}{a} + H_{pq}\frac{q\pi}{b}\right]$$
$$C_{pq} = K\left[E_{pq}\frac{q\pi}{b} - H_{pq}\frac{p\pi}{a}\right] \qquad (8)$$

where E_{pq} and H_{pq} are the mode amplitude coefficients for the pq^{th} TE and TM modes, respectively. The quantity K is one which could have been incorporated into E_{pq} and H_{pq}. The substitution of Equations (8) into (1), (2a), and (2b) is quite straightforward, but does not lead to any simplification. On the contrary, the resulting equations are even more unwieldy.

The next effort, directed toward finding an analytical convergence criterion for the simultaneous equations, was an attempt to derive an expression that would relate the change in the admittance to the change in the mode amplitude coefficients. If this is accomplished by taking the derivative of Equations (1), (2a), and (2b) with respect to the coefficients, considering the admittance to be a member of the group, the result is a matrix whose determinant should approach a constant value as the number of modes is increased. This, however, is almost identical to solving the matrix for Equations (2a) and (2b), substituting the obtained values for the mode amplitude coefficients into Equation (1), and then insisting that the admittance "Y" must approach a constant value. Consequently, this effort was also abandoned.

TABLE 9

E-PLANE CUT ON A SQUARE GRID ARRAY OF SQUARE WAVEGUIDES;
COMPARISON OF ADVANCED THEORY WITH THE SIMPLE GRATING LOBE SERIES

	Simple Grating Lobe Series		Advanced Theory	
Y	G	B	G	B
0.500	1.102326	0.0427453	-	-
0.510	1.096260	0.563385	-	-
0.520	1.090177	0.751856	0.395083	1.153299
0.530	1.084084	1.044166	0.271361	1.608455
0.540	1.077990	1.612427	0.087137	2.584137
0.550	1.071903	4.065890	0.947626	8.063701
0.560	4.017475	-0.439213	4.032689	0.302194
0.570	3.027679	-0.436978	3.115006	0.199048
0.580	2.668593	-0.434826	-	-
0.590	2.472502	-0.432759	-	-
0.600	2.346421	-0.430781	-	-

It was decided to attack the problem on a numerical basis. To do so, the defining equations for the admittance and mode amplitude coefficients were programmed for computer solution in such a way as to include the possibility of exciting all dominant polarization and all cross-polarization higher order LSE waveguide modes which have either eigennumber of the defining pair (p, q) equal to or less than 4 and including zero. As a consequence, there are 19 "dominant" and 20 "cross" higher order modes to be considered inside the waveguides. In the array-space region is was decided, on the basis of the information presented in the unshaded portion of Figure 2, that the range of the external eigennumbers should be $-30 \leq m \leq 30$, $-30 \leq n \leq 30$ in order to adequately accommodate either internal eigennumber (p or q) being equal to 4. This gives a total of 3721 external modes being taken into account.

The output data at each point in sine theta space consisted of the complex amplitude coefficient for each mode and the associated contribution to the radiation admittance as well as the absolute value of their product. Since the mode amplitude coefficient is essentially equivalent to voltage, the product of mode amplitude coefficient and mode admittance contribution has the units of current. This last was computed because it was felt that since the mode contributions are essentially admittances in parallel, then those modes having the greatest current would be the ones of greatest importance. That this concept is not valid can be seen by considering the P, Q = 2, 4 mode which from Table 10 has an |AMP*Y| = 0.0637. Note that the mode P, Q = 1, 2 has an |AMP*Y| = 0.3632. If now the mode amplitude coefficients for these two modes are compared, we find that they are not too different and, in fact, the former is the larger. Suppose a selection criterion were assumed where only those modes having an |AMP*Y| greater than five percent of that of the dominant mode (P, Q = 1, 0) were to be considered. Obviously the P, Q = 2, 4 mode would be dropped from consideration. This, however, would be an error because Equations (2) show that the amplitude of any one mode is a function of the values of all of the others. Consequently, in any process of truncation of the infinite set of simultaneous equations, the omission of any mode having a substantial amplitude coefficient will very adversely affect the accuracy of all of the others, upon solution of the truncated set. The same argument holds for rejecting the possible selection criterion based upon the amplitude of the mode contribution to the radiation admittance.

The remaining quantity suitable for selection is the mode amplitude coefficient itself. A few trial-and-error manipulations suggested that the best way to handle the selection was to work with the square of the absolute value. That this is a pertinent choice may be recognized by noting that the waveguide mode energy is equal to the square of the mode voltage amplitude coefficient times the wave admittance, the latter of which is a quantity varying approximately inversely as the propagation constant. Since, from Table 1, the propagation constants for the modes of interest are all of roughly the same order, we can safely ignore them for our purposes. Squaring the value automatically tends to enhance the larger amplitude values and to very sharply suppress those that are small. It was decided to select on the basis of the results obtained for the maximum number of modes that could be accommodated by the available computer (IBM 7094). The computer runs were made at a single point in each of H-plane, E-plane, and one intermediate plane for each of three grid sizes

TABLE 10

MODE ADMITTANCE CONTRIBUTIONS FOR A TRIANGULAR GRID ARRAY AT H-PLANE SIN Θ = 0.5

P Q	AMPR	AMPI	G	B	|AMP*Y|
Dominant Mode Contribution					
1 0	1.0000	0.0000	0.8098	1.7858	1.9609
Principal Polarization Contributions					
2 0	0.1945	1.5837	-0.7289	2.0892	3.5305
2 4	-0.0660	-1.2233	0.0028	0.0519	0.0637
1 2	0.0507	1.0464	-0.0168	-0.3463	0.3632
2 2	-0.0776	-0.8977	-0.0136	-0.1574	0.1423
1 4	-0.0269	-0.5858	-0.0024	-0.0524	0.0308
4 2	-0.	0.0959	0.	-0.0066	0.0006
4 0	0.0425	-0.0841	-0.0447	0.0347	0.0053
3 0	0.0133	0.0454	0.0053	0.0092	0.0005
3 4	0.	0.0126	0.	0.0001	0.
3 2	0.	-0.0192	0.	-0.0006	0.
Cross-Polarization Contributions					
2 2	0.0162	0.2496	-0.0018	-0.0284	0.0071
0 2	-0.0076	-0.1432	0.0039	0.0730	0.0105
4 2	-0.0004	-0.0995	-0.	-0.0033	0.0003
1 2	-0.0036	-0.0443	-0.0018	-0.0223	0.0010
0 4	0.0018	0.0330	0.0004	0.0081	0.0003
3 2	-0.0005	0.0112	0.	0.0002	0.
1 4	0.0010	0.0126	-0.0003	-0.0035	0.

a/λ = 0.905 b/λ = 0.400 A/λ = 1.008 B/λ = 1.008

AMPR = real part of mode amplitude coefficient
AMPI = imaginary part of mode amplitude coefficient
G = radiation conductance
B = radiation susceptance
AMP*Y= product of amplitude coefficient and admittance

for both rectangular and triangular grid. For each plane, the values for each grid size corresponding to a given mode were added, in order to obtain a composite value valid for several grids and waveguide sizes. Doing this will also tend to average out small variations in the order for one grid size relative to another. The mode order for that scan plane was determined by the value of that mode's sum in relation to the other mode sums. These data are shown in Tables 11, 12, and 13 for the triangular grid and in Tables 15, 16, and 17 for the rectangular grid. Tables 14 and 18 are the final mode order for each of the three scan planes for the triangular grid and the rectangular grid, respectively.

The problem at this point is to effectively use the data presented in Tables 14 and 18. It was decided that if a value for a mode in the two tables above exceeded one percent of the Dominant Mode (TE_{10}) value of 3.0, then that mode should be included in the set for the simultaneous solution of Equations (2) after truncation. This one percent level is indicated by the short line in each column in both tables. The modes were accordingly incorporated into the computer program. Table 10 is an excerpt from the 19 "dominant" and 20 "cross" case for an H-plane point. Table 19 is a similar table for the same H-plane point except that the modes are limited to those specified by Table 14 for the triangular grid. Table 10, if it were all present, would give a total radiation admittance of $Y = 0.011997 + j\ 3.429789$. Table 19 gives $Y = 0.030419 + j\ 3.238305$. The difference between these amounts to an error in the absolute value of less than six percent. For the same grid at an E-plane point ($x = 0$, $y = 0.5$), the 19 and 20 gives $Y = 1.602131 + j\ 0.221731$ and the modes of Table 14 give $Y = 1.594270 + j\ 0.219018$. At an intercardinal point ($x = 0.23$, $y = 0.23$) not far from the grating lobe circle, the results are, for the 19 and 20, $Y = 0.283723 + j\ 1.826422$ versus $Y = 0.342088 + j\ 1.329688$ for the suggested number of modes. The error for the intercardinal point is about 24.6 percent in the absolute value of the admittance. This could easily be improved by including only a few more modes from the table for the mode order (Table 14).

The suggested number of modes (Table 18) was tested by making an E-plane cut for a rectangular grid as shown in Figure 4. This is the same array and the same cut that was discussed in association with Tables 8 and 9 in the last paragraph of the previous section. It was pointed out that the notch shown in Table 3 by the "Advanced Theory" is an anomalous

TABLE 11

TRIANGULAR GRID MODE COMPARISON BASED UPON MODE AMPLITUDE SQUARED FOR H-PLANE SCAN

X = H-plane sin Θ

P Q	$a/\lambda=0.905, b/\lambda=0.4$ $A/\lambda=1.008, B/\lambda=1.008$ X = 0.5, Y=0	$a/\lambda=0.75, b/\lambda=0.333$ $A/\lambda=0.8333, B/\lambda=0.833$ X = 0.7, Y=0	$a/\lambda=0.6364, b/\lambda=0.2828$ $A/\lambda=0.7071, B/\lambda=0.7071$ X = 0.7, Y=0	Sum*
Principal Polarization				
1 1	0.	0.	0.	0.
2 0	2.5459	0.1258	0.0409	2.7126
1 2	1.0976	0.2608	0.1356	1.3993
3 0	0.0023	0.0029	0.0009	0.0061
1 3	0.	0.	0.	0.
1 4	0.3437	0.0912	0.0514	0.4863
3 1	0.	0.	0.	0.
2 2	0.8119	0.0605	0.0267	0.8991
2 1	0.	0.	0.	0.
4 0	0.0089	0.0020	0.0008	0.0117
2 4	1.5009	0.0063	0.0082	1.5154
3 2	0.0004	0.	0.	0.
4 1	0.	0.	0.	0.
3 3	0.	0.	0.	0.
2 3	0.	0.	0.	0.
4 2	0.0092	0.0035	0.0021	0.0148
3 4	0.0002	0.0004	0.	0.0006
4 3	0.	0.	0.	0.
Cross-Polarization				
1 1	0.	0.	0.	0.
0 1	0.	0.	0.	0.
3 1	0.	0.	0.	0.
2 1	0.	0.	0.	0.
1 2	0.0020	0.0014	0.0001	0.0035
0 2	0.0205	0.0022	0.0009	0.0236
2 2	0.0626	0.0069	0.0029	0.0724
4 1	0.	0.	0.	0.
1 3	0.	0.	0.	0.
3 2	0.0001	0.0007	0.	0.0008
4 2	0.0099	0.0033	0.0016	9.0148
3 3	0.	0.	0.	0.
1 4	0.0002	0.0001	0.	0.0002
0 4	0.0011	0.0001	0.	0.0012
3 4	0.	0.	0.	0.
0 3	0.	0.	0.	0.
2 3	0.	0.	0.	0.

* Sum of the Three Grids PQ^{th} Mode Value

one because it is occurring inside of the grating lobe onset position and of the notch predicted by the simple grating lobe series. Insofar as the experimental curve is concerned, all that can be said is that the "Advanced Theory" agrees with the experiment better than does the simple grating lobe series. This poor agreement may be due to the array being too small even at 13 x 13.

The suggested number of modes (Table 14) was tested by making an H-plane cut for a triangular grid, as shown in Figure 5. Here the anomalous notch is far enough inside the H-plane onset position of the grating lobe that it is readily obvious. There are three "Advanced Theory" predictions depicted on this figure, all of which predict a notch. The curve for one dominant and no cross modes is with the TE_{20} mode only. The curve with five dominant and one cross is the suggested list to the lines (Table 14), and the predicted notch is somewhat farther out in sine theta space. The other curve is the first eight dominant and the first seven cross from the suggested list and predicts a notch nearly like that of the TE_{20} only. It is apparent from this result that selecting the modes only to the one-percent level in Table 14 is inadequate to give a stationary prediction for the notch even though the radiation admittance is relatively stationary.

TABLE 12

MODE COMPARISON BASED UPON MODE AMPLITUDE SQUARED
FOR E-PLANE SCAN

Y = E-plane sin Θ

P Q	$a/\lambda=0.905, b/\lambda=0.4$ $A/\lambda=1.008, B/\lambda=1.008$ X = 0, Y = 0.5	$a/\lambda=0.75, b/\lambda=0.333$ $A/\lambda=0.8333, B/\lambda=0.8333$ X = 0, Y = 0.7	$a/\lambda=0.6364, b/\lambda=0.2828$ $A/\lambda=0.7071, B/\lambda=0.7071$ X = 0, Y = 0.7	Sum*
Principal Polarization				
1 1	0.1676	0.1862	0.2393	0.5931
2 0	0.	0.	0.	0.
1 2	0.0736	0.0929	0.0796	0.2461
3 0	0.0780	0.0122	0.0099	0.1001
1 3	0.0207	0.0309	0.0424	0.0940
1 4	0.0314	0.0357	0.0317	0.0987
3 1	0.0138	0.0113	0.0108	0.0359
2 2	0.	0.	0.	0.
2 1	0.	0.	0.	0.
4 0	0.	0.	0.	0.
2 4	0.	0.	0.	0.
3 2	0.0048	0.0023	0.0029	0.0100
4 1	0.	0.	0.	0.
3 3	0.0060	0.0044	0.0032	0.0136
2 3	0.	0.	0.	0.
4 2	0.	0.	0.	0.
3 4	0.0013	0.0008	0.0009	0.0030
4 3	0.	0.	0.	0.
Cross-Polarization				
1 1	0.1682	0.1574	0.1082	0.4338
0 1	0.	0.	0.	0.
3 1	0.0449	0.0515	0.0401	0.1365
2 1	0.	0.	0.	0.
1 2	0.0016	0.0023	0.0021	0.0060
0 2	0.	0.	0.	0.
2 2	0.	0.	0.	0.
4 1	0.	0.	0.	0.
1 3	0.0018	0.0017	0.0014	0.0050
3 2	0.0008	0.0017	0.0015	0.0040
4 2	0.	0.	0.	0.
3 3	0.0004	0.0006	0.0006	0.0016
1 4	0.	0.0001	0.0001	0.0002
0 4	0.	0.	0.	0.
3 4	0.	0.0001	0.0001	0.0002
0 3	0.	0.	0.	0.
2 3	0.	0.	0.	0.

*Sum of the Three Grids PQ^{th} Mode Value

TABLE 13

TRIANGULAR GRID MODE COMPARISON BASED UPON MODE AMPLITUDE SQUARED FOR INTERCARDINAL SCAN

P Q	a/λ=0.905, b/λ=0.4 A/λ=1.008, B/λ=1.008 X = 0.23, Y = 0.23	a/λ=0.75, b/λ=0.333 A/λ=0.8333, B/λ=0.8333 X = 0.4, Y = 0.4	a/λ=0.6364, b/λ=0.2828 A/λ=0.7071, B/λ=0.7071 X = 0.5, Y = 0.5	Sum*
Principal Polarization				
1 1	0.5519	0.2312	0.1950	0.9781
2 0	2.6034	0.1814	0.0525	2.8373
1 2	0.3629	0.1233	0.0812	0.5674
3 0	0.0193	0.0025	0.0017	0.0235
1 3	0.0850	0.0388	0.0338	0.1576
1 4	0.1151	0.0473	0.0342	0.1966
3 1	0.0060	0.0007	0.0014	0.0081
2 2	0.8334	0.0777	0.0276	0.9387
2 1	0.2108	0.0242	0.0117	0.2467
4 0	0.0037	0.0018	0.0010	0.0065
2 4	0.2213	0.0006	0.0093	0.2312
3 2	0.0097	0.0015	0.0008	0.0120
4 1	0.0006	0.0010	0.0015	0.0031
3 3	0.0004	0.0004	0.0004	0.0012
2 3	0.0489	0.0078	0.0044	0.0611
4 2	0.0037	0.0022	0.0014	0.0073
3 4	0.0026	0.0004	0.0002	0.0032
4 3	0.0003	0.0006	0.0008	0.0017
Cross-Polarization				
1 1	0.1175	0.0049	0.0091	0.1315
0 1	0.0576	0.0092	0.0101	0.0769
3 1	0.0100	0.0028	0.0040	0.0168
2 1	0.0770	0.0133	0.0162	0.1065
1 2	0.0120	0.0007	0.0002	0.0129
0 2	0.0070	0.0015	0.0007	0.0092
2 2	0.0199	0.0044	0.0020	0.0263
4 1	0.0078	0.0064	0.0084	0.0226
1 3	0.0007	0.0001	0.0001	0.0009
3 2	0.0030	0.0003	0.0002	0.0035
4 2	0.0030	0.0018	0.0010	0.0058
3 3	0.	0.0001	0.0001	0.0002
1 4	0.0004	0.	0.	0.0004
0 4	0.0004	0.	0.	0.0004
3 4	0.0001	0.	0.	0.0001
0 3	0.0004	0.0001	0.0001	0.0006
2 3	0.	0.0003	0.0003	0.0006

* Sum of the Three Grids PQ^{th} Mode Value

TABLE 14

TRIANGULAR GRID MODE ORDER

Order	H-Plane Scan		E-Plane Scan		Intercardinal Scan	
	P Q	Sum	P Q	Sum	P Q	Sum
Dominant Mode						
0	10	3.0000	10	3.0000	10	3.0000
Principal Polarization						
1	20	2.7126	11	0.5931	20	2.8373
2	24	1.5154	12	0.2461	11	0.9781
3	12	1.3993	30	0.1001	22	0.9387
4	22	0.8991	14	0.0987	12	0.5674
5	14	0.4863	13	0.0940	21	0.2467
6	42	0.0.48	31	0.0359	24	0.2312
7	40	0.0117	33	0.0136	14	0.1966
8	30	0.0061	32	0.0100	13	0.1576
9	34	0.0006	34	0.0030	23	0.0611
10	32	0.0004			30	0.0235
11					32	0.0120
12					31	0.0081
13					42	0.0073
14					40	0.0065
15					34	0.0032
16					41	0.0031
17					43	0.0017
Cross-Polarization						
1	22	0.0724	11	0.4338	11	0.1315
2	02	0.0236	31	0.1365	21	0.1065
3	42	0.0148	12	0.0060	01	0.0769
4	12	0.0035	13	0.0050	22	0.0263
5	04	0.0012	32	0.0040	41	0.0226
6	32	0.0008	33	0.0016	31	0.0168
7	14	0.0002	14	0.0002	12	0.0129
8			34	0.0002	02	0.0092
9					42	0.0058
10					32	0.0035
11					13	0.0009
12					03	0.0006
13					23	0.0006
14					14	0.0004
15					04	0.0004
16					33	0.0002
17					34	0.0001

TABLE 15

RECTANGULAR GRID MODE COMPARISON BASED UPON MODE AMPLITUDE SQUARED FOR H-PLANE SCAN

X = H-plane sin Θ

P Q	$a/\lambda=0.6, b/\lambda=0.2667$ $A/\lambda=0.666, B/\lambda=0.333$ X = 0.4, Y = 0	$a/\lambda=0.5898, b/\lambda=0.5898$ $A/\lambda=0.6439, B/\lambda=0.6439$ X = 0.5, Y= 0	$a/\lambda=0.6364, b/\lambda=0.6364$ $A/\lambda=0.7071, B/\lambda=0.7071$ X = 0.375, Y = 0	Sum*
Principal Polarization				
1 1	0.	0.	0.	0.
1 2	0.0155	0.0042	0.0058	0.0255
1 4	0.0083	0.0028	0.0037	0.0148
1 3	0.	0.	0.	0.
2 0	0.0069	0.0105	0.0412	0.0586
4 0	0.0002	0.0003	0.0003	0.0008
2 1	0.	0.	0.	0.
3 0	0.0014	0.0011	0.0017	0.0042
3 1	0.	0.	0.	0.
3 2	0.	0.	0.	0.
2 2	0.0001	0.	0.	0.0001
2 3				
4 2				
4 1				
3 3				
4 3				
2 4				
3 4				
Cross-Polarization				
1 1	0.	0.	0.	0.
3 1	0.	0.	0.	0.
1 2	0.	0.	0.0002	0.0002
0 1				
2 1				
3 2				
4 1				
1 4				
2 2				
0 2				
1 3				
3 3				
3 4				
2 3				
4 2				
0 3				
4 3				

*Sum of the Three Grids PQ^{th} Mode Value

TABLE 16

RECTANGULAR GRID MODE COMPARISON BASED UPON MODE AMPLITUDE SQUARED FOR E-PLANE SCAN

Y = E-plane sin Θ

P Q	a/λ=0.6, b/λ=0.2667 A/λ=0.666, B/λ=0.333 X = 0, Y = 0.4	a/λ=0.5898, b/λ=0.5898 A/λ=0.6439, B/λ=0.6439 X = 0, Y = 0.5	a/λ=0.6364, b/λ=0.6364 A/λ=0.7071, B/λ=0.7071 X = 0, Y = 0.375	Sum*
Principal Polarization				
1 1	0.0196	0.3919	5.8252	6.2367
1 2	0.0190	0.2671	1.3283	1.6144
1 4	0.0098	0.1079	0.4900	0.7669
1 3	0.0044	0.0397	0.5256	0.5697
2 0	0.	0.	0.	0.
4 0	0.	0.	0.	0.
2 1	0.	0.	0.	0.
3 0	0.0036	0.0056	0.0123	0.0215
3 1	0.0026	0.0015	0.0190	0.0232
3 2	0.0001	0.0016	0.0111	0.0128
2 2	0.	0.	0.	0.
2 3	0.	0.	0.	0.
4 2	0.	0.	0.	0.
4 1	0.	0.	0.	0.
3 3	0.0006	0.	0.0004	0.0010
4 3	0.	0.	0.	0.
2 4	0.	0.	0.	0.
3 4	0.	0.	0.0086	0.
Cross-Polarization				
1 1	0.0164	1.6377	10.8756	12.5297
3 1	0.0056	0.2214	1.1537	1.3807
1 2	0.0001	0.0749	0.5255	0.6005
0 1	0.	0.	0.	0.
2 1	0.	0.	0.	0.
3 2	0.	0.0254	0.1723	0.1977
4 1	0.	0.	0.	0.
1 4	0.	0.0025	0.0146	0.0171
2 2	0.	0.	0.	0.
0 2	0.	0.	0.	0.
1 3	0.0003	0.0006	0.0071	0.0080
3 3	0.	0.0007	0.0111	0.0118
3 4	0.	0.0020	0.0111	0.0131
2 3	0.			
4 2				
0 3				
4 3				

*Sum of the Three Grids PQ^{th} Mode Value

TABLE 17

RECTANGULAR GRID MODE COMPARISON BASED UPON MODE AMPLITUDE SQUARED FOR INTERCARDINAL SCAN

P Q	$a/\lambda=0.6, b/\lambda=0.2667$ $A/\lambda=0.666, B/\lambda=0.333$ X = 0.4, Y = 0.4	$a/\lambda=0.5898, b/\lambda=0.5898$ $A/\lambda=0.6349, B/\lambda=0.6439$ X = 0.5, Y = 0.5	$a/\lambda=0.6364, b/\lambda=0.6364$ $A/\lambda=0.7071, B/\lambda=0.7071$ X = 0.375, Y = 0.375	Sum*
Principal Polarization				
1 1	0.0179	0.1093	0.8665	0.9937
1 2	0.0221	0.1353	0.2417	0.3991
1 4	0.0112	0.0515	0.0861	0.1488
1 3	0.0049	0.0211	0.0917	0.1177
2 0	0.0093	0.0083	0.0049	0.0225
4 0	0.0003	0.0002	0.0001	0.0006
2 1	0.0157	0.0009	0.0026	0.0192
3 0	0.0015	0.0013	0.0018	0.0046
3 1	0.0018	0.	0.0001	0.0019
3 2	0.	0.0002	0.0001	0.0003
2 2	0.0014	0.0030	0.0012	0.0056
2 3	0.0035	0.0008	0.0016	0.0059
4 2	0.	0.0001	0.	0.0001
4 1	0.0008	0.	0.	0.0008
3 3	0.0004	0.	0.	0.0004
4 3	0.0003	0.	0.	0.0003
2 4	0.0005	0.0010	0.0004	0.0019
3 4	0.	0.0001	0.	0.0001
Cross-Polarization				
1 1	0.0117	0.1704	0.9403	1.1224
3 1	0.0037	0.0129	0.0681	0.0847
1 2	0.	0.0038	0.0064	0.0102
0 1	0.0053	0.1302	0.1996	0.3351
2 1	0.0087	0.0609	0.1393	0.2089
3 2	0.	0.0011	0.0033	0.0044
4 1	0.0033	0.0163	0.0404	0.0600
1 4	0.	0.0002	0.	0.0002
2 2	0.	0.0035	0.0032	0.0067
0 2	0.	0.0024	0.0054	0.0078
1 3	0.0002	0.0003	0.0003	0.0008
3 3	0.	0.	0.0002	0.0002
3 4	0.	0.	0.0001	0.0001
2 3	0.0002	0.0002	0.0001	0.0005
4 2	0.	0.0010	0.0008	0.0018
0 3	0.	0.0001	0.	0.0001
4 3	0.	0.	0.	0.

*Sum of the Three Grids PQ^{th} Mode Value

TABLE 18

RECTANGULAR GRID MODE ORDER

Order	H-Plane Scan		E-Plane Scan		Intercardinal Scan	
	P Q	Sum	P Q	Sum	P Q	Sum
Dominant Mode						
0	10	3.0000	10	3.0000	10	3.0000
Principal Polarization						
1	20	0.0586	11	6.2367	11	0.9937
2	12	0.0255	12	1.6144	12	0.3991
3	14	0.0148	14	0.7669	14	0.1488
4	30	0.0042	13	0.5697	13	0.1177
5	40	0.0008	31	0.0232	20	0.0225
6	22	0.0001	30	0.0215	21	0.0192
7			32	0.0128	23	0.0059
8			33	0.0010	22	0.0056
9					30	0.0046
10					31	0.0019
11					24	0.0019
12					41	0.0008
13					40	0.0006
14					33	0.0004
15					32	0.0003
16					43	0.0003
17					42	0.0001
Cross-Polarization						
1	12	0.0002	11	12.5297	11	1.1224
2			31	1.3807	01	0.3351
3			12	0.6005	21	0.2089
4			32	0.1977	31	0.0847
5			14	0.0171	41	0.0600
6			34	0.0131	12	0.0102
7			33	0.0118	02	0.0078
8			13	0.0080	22	0.0067
9					32	0.0044
10					42	0.0018
11					13	0.0008
12					23	0.0005
13					14	0.0002
14					33	0.0002
15					34	0.0001
16					24	0.0001
17						

TABLE 19

MODE ADMITTANCE CONTRIBUTIONS FOR A TRIANGULAR GRID ARRAY AT H-PLANE $\sin \Theta = 0.5$

$\frac{a}{\lambda} = 0.905 \quad \frac{b}{\lambda} = 0.400 \quad \frac{A}{\lambda} = 1.008 \quad \frac{B}{\lambda} = 1.008$

P Q	AMPR	AMPI	G	B
Dominant Mode Contribution				
1 0	1.0000	0.0000	0.8098	1.7858
Principal Polarization Contributions				
2 0	0.1490	1.5292	-0.7520	1.9935
2 4	-0.0526	-1.2811	0.0022	0.0544
1 2	0.0477	1.1052	-0.0158	-0.3658
2 2	-0.0574	-0.8268	-0.0101	-0.1449
1 4	-0.0265	-0.6495	-0.0024	-0.0581
Cross-Polarization Contributions				
2 2	0.0119	0.2336	-0.0014	-0.0265

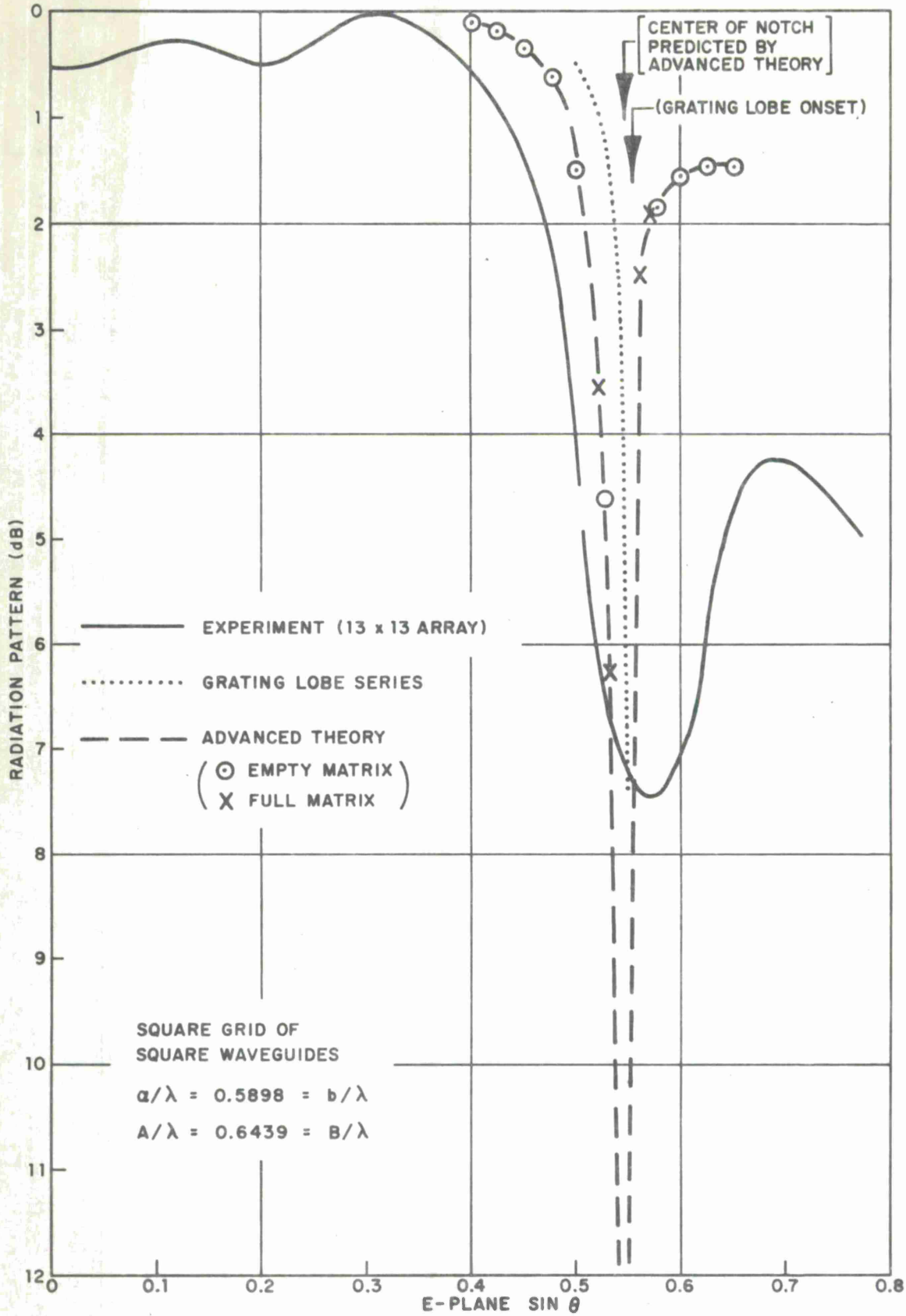

Figure 4. Comparison of Theory and Experiment for an E-Plane Scan of an Array of Square Waveguides on a Square Grid

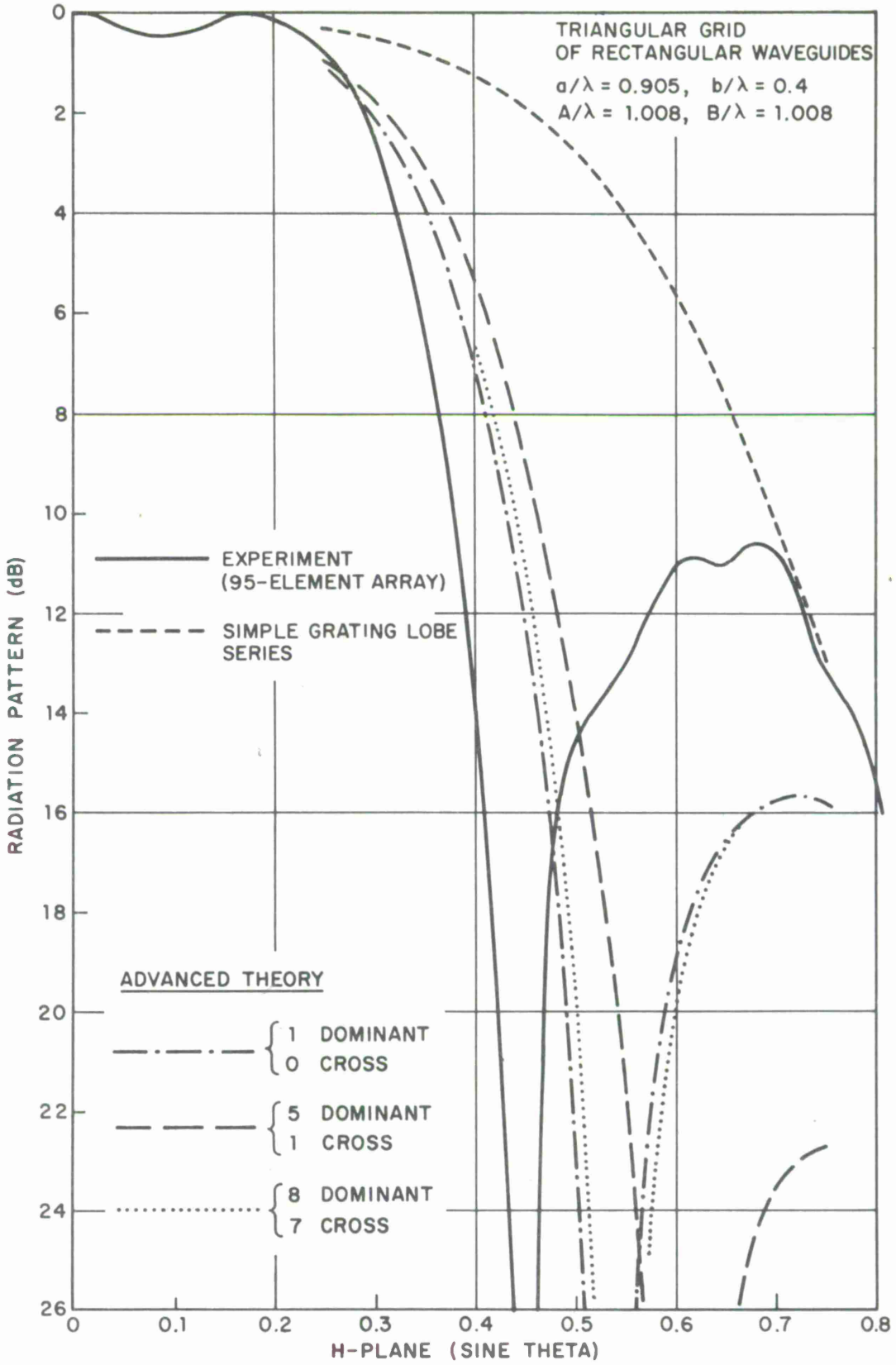

Figure 5. Comparison of Theory and Experiment for an H-Plane Scan of an Array of Rectangular Waveguides on a Triangular Grid

SECTION V

CONCLUSIONS

The waveguide higher order modes in the order of decreasing importance are given in Tables 14 and 18 for triangular grid and rectangular grid, respectively. These tables were compiled on the basis of the square of the absolute value of the mode amplitude coefficients obtained from solutions of simultaneous equations having 19 dominant polarization and 20 cross-polarization modes. The short lines in the columns represent the one-percent level as compared with the incident mode amplitude.

The foremost conclusion is that even for grids giving sharply restricted fields of view, the number of modes necessary for a reasonably accurate representation of the radiation admittance is not excessively great even for an intercardinal point. The worst case situation, of intercardinal scan of a triangular grid, calls for about nine principal polarization higher order LSE modes and about three cross-polarization LSE modes. For this case the expected running time for the available computer program is approximately 1.25 minutes per point in sine theta space. In regions about E- and H-planes for the triangular grid and about E-plane for the rectangular grid, about eight higher order modes are necessary, for which the expected running time should be about 0.8 minute. The region about H-plane scan for the rectangular grid requires only the TE_{20} mode. For a region around broadside, the simple grating lobe series alone is adequate. At the present time there is not enough information available to determine how far off from E-plane (for example) one may go and still safely continue to use the E-plane family of modes. The same situation holds true of course for the extent of a "broadside" region and an "H-plane" region. This is an area of investigation that is suggested for future work.

The mode numbers mentioned above are those above the one-percent level of the square of the mode amplitude coefficient. This level appears to be adequate for predicting a relatively stationary radiation admittance, but the notch position is apparently very sensitive to the value of the radiation admittance and so a greater number of modes is necessary if the position of the notch is to be predicted accurately. The minimum number of modes necessary to predict the position of notch with confidence is not known and should be investigated further.

The analytical and numerical work concerning the range over which the external eigennumbers should extend shows that if an eigennumber of the pair for the internal waveguide modes is equal to 4 then the associated external eigennumber should have a range of ±30. At the present time, the available computer program is written to take the most conservative view that if any internal mode has either eigennumber of the pair equal to 4, then both external eigennumbers should have a range of ±30 for all members of the matrix for the simultaneous equations. For example, the matrix element for which P, Q = 4, 2 and p, q = 1, 2 is currently computed with $-30 \leq \begin{matrix} m \\ n \end{matrix} \leq 30$ and so has 3720 terms in the double sum for the element. Reference to Figure 2 indicates that with P = 4 and p = 1, then M = 14, so $-14 \leq m \leq 14$, and with Q = 2 and q = 2 then N = 10 so $-10 \leq n \leq 10$. So doing would give only 609 terms in the double sum for that same element. This possible reduction in labor and computer running time should be investigated further.

SECTION VI

REFERENCES

1. Edelberg, S., and Oliner, A.A., "Mutual Coupling Effects in Large Antenna Arrays: Part I - Slot Arrays," IRE Transactions on Antennas and Propagation, Vol. AP-8, pp. 286-297, May 1960.

2. Farrell, G.F. Jr., and Kuhn, D.H., "Mutual Coupling Effects of Triangular-Arrays by Modal Analysis," IEEE Transactions on Antennas and Propagation, Vol. AP-14, pp. 652-654, September 1966.

3. This experimental curve was furnished by courtesy of Lincoln Laboratory, Lexington, Massachusetts.

APPENDIX A

DERIVATION OF THE MUTUAL COUPLING IN AN INFINITE ARRAY OF RECTANGULAR WAVEGUIDE HORNS

The problem is solved by constructing Fourier Series expansions in terms of the normal modes for the field components in both the free space region and in the element waveguide. Both TE and TM modes are required in the free space region to account for the total far-field distribution (Ref. 1), and are included in the free space Fourier representation. For completeness, both TE and TM modes are also included in the waveguide series expansion. Fourier methods are then employed to enforce the continuity of the total fields across the boundary of the face of the array.

The radiation admittance equation as obtained by this method consists of the so-called grating lobe series for the dominant mode of the waveguide, plus correction terms. Each correction term is the product of a higher order waveguide mode amplitude coefficient and a series having a form similar to the grating lobe series. The higher order waveguide mode amplitude coefficients are obtained from the solution of a family of simultaneous equations which are derived concurrently with the admittance equation. It is obvious, therefore, that the problem may not be solved exactly, because in practice one is forced to truncate the grating lobe series, and there is also a practical limit to the number of waveguide modes that one would with to consider. Fortunately, the range of eigennumbers over which the grating lobe series needs to be summed is not excessively large, and only a few waveguide modes need to be considered in order to obtain reasonable accuracy.

Figures 1a and 1b show the rectangular array and triangular array, respectively. In both cases the unit cell is outlined by a rectangle, the dimensions of which are the units of the lattice periodicity in the two directions. Since the lattice is periodic, each mode of the field in the free space region of the array has a form governed by Floquet's theorem. A suitable form is

$$e^{-j\left[k_x + \frac{2m\pi}{A}\right]x} e^{-j\left[k_y + \frac{2n\pi}{B}\right]y} e^{\mp\Gamma_{mn}z} \qquad \text{(A-1)}$$

where

$$k_x = k_o \sin\Theta\cos\psi$$

$$k_y = k_o \sin\Theta\sin\psi$$

$$k_o = \frac{2\pi}{\lambda_o}$$

and where $k_x A$ and $k_y B$ are the phase shifts between adjacent lattice units in the x and y directions, respectively.

A phenomenological visualization of the fields above the surface of the array for the case of arbitrary scan indicates that all three components of electric and magnetic fields could be present. This condition is most easily handled by making a linear combination of TE and TM fields. Let V_{mn} and M_{mn} be the respective mode amplitude coefficients for the TE_{mn} and TM_{mn} fields, and for ease in writing let

$$\beta_m = k_x + \frac{2m\pi}{A}$$
$$\beta_n = k_y + \frac{2n\pi}{B} \qquad \text{(A-2)}$$

The six components of the combined $TE\text{-}TM_{mn}$ or EM_{mn} mode are

$$E_x = -(V_{mn}\beta_n - M_{mn}\beta_m)\, e^{-j\beta_m x} e^{-j\beta_n y} e^{\mp\Gamma_{mn} z}$$
$$E_y = (V_{mn}\beta_m + M_{mn}\beta_n)\, e^{-j\beta_m x} e^{-j\beta_n y} e^{\mp\Gamma_{mn} z}$$
$$E_z = \mp j\, M_{mn} \frac{\beta_m^2 + \beta_n^2}{\Gamma_{mn}} e^{-j\beta_m x} e^{-j\beta_n y} e^{\mp\Gamma_{mn} z} \qquad \text{(A-3)}$$
$$H_x = \mp\left[V_{mn}\beta_m \frac{\Gamma_{mn}}{j\omega\mu} + M_{mn}\beta_n \frac{j\omega\epsilon_o}{\Gamma_{mn}}\right] e^{-j\beta_m x} e^{-j\beta_n y} e^{\mp\Gamma_{mn} z}$$
$$H_y = \mp\left[V_{mn}\beta_n \frac{\Gamma_{mn}}{j\omega\mu} - M_{mn}\beta_m \frac{j\omega\epsilon_o}{\Gamma_{mn}}\right] e^{-j\beta_m x} e^{-j\beta_n y} e^{\mp\Gamma_{mn} z}$$
$$H_z = j\, V_{mn} \frac{\beta_m^2 + \beta_n^2}{j\omega\mu} e^{-j\beta_m x} e^{-j\beta_n y} e^{\mp\Gamma_{mn} z}$$

where a time dependence of $\exp(j\omega t)$ is understood and

$$\Gamma_{mn} = k_o \sqrt{\left[\frac{\beta_m}{k_o}\right]^2 + \left[\frac{\beta_n}{k_o}\right]^2 - 1} \qquad \text{(A-4)}$$

The upper sign of the double signs where they occur designates propagation in the positive z direction.

Six components of field can also be expected inside the aperture of the element waveguide, and will be treated as a linear combination of TE and TM modes with respective mode amplitude coefficients E_{pq} and H_{pq}. The six field components have the form

$$
\begin{aligned}
E_x &= -\left[E_{pq}\,\frac{q\pi}{b} - H_{pq}\,\frac{p\pi}{a}\right]\cos\frac{p\pi x}{a}\sin\frac{q\pi y}{b}\,e^{\mp\gamma_{pq}z} \\
E_y &= \left[E_{pq}\,\frac{p\pi}{a} + H_{pq}\,\frac{q\pi}{b}\right]\sin\frac{p\pi x}{a}\cos\frac{q\pi y}{b}\,e^{\mp\gamma_{pq}z} \\
E_z &= \mp H_{pq}\,\frac{\left[\frac{p\pi}{a}\right]^2 + \left[\frac{q\pi}{b}\right]^2}{\gamma_{pq}}\sin\frac{p\pi x}{a}\sin\frac{q\pi y}{b}\,e^{\mp\gamma_{pq}z} \\
H_x &= \mp\left[E_{pq}\,\frac{p\pi}{a}\,\frac{\gamma_{pq}}{j\omega\mu} + H_{pq}\,\frac{q\pi}{b}\,\frac{j\omega\epsilon_r}{\gamma_{pq}}\right]\sin\frac{p\pi x}{a}\cos\frac{q\pi y}{b}\,e^{\mp\gamma_{pq}z} \\
H_y &= \mp\left[E_{pq}\,\frac{q\pi}{b}\,\frac{\gamma_{pq}}{j\omega\mu} - H_{pq}\,\frac{p\pi}{a}\,\frac{j\omega\epsilon_r}{\gamma_{pq}}\right]\cos\frac{p\pi x}{a}\sin\frac{q\pi y}{b}\,e^{\mp\gamma_{pq}z} \\
H_z &= -E_{pq}\,\frac{\left[\frac{p\pi}{a}\right]^2 + \left[\frac{q\pi}{b}\right]^2}{j\omega\mu}\cos\frac{p\pi x}{a}\cos\frac{q\pi y}{b}\,e^{\mp\gamma_{pq}z}
\end{aligned}
\qquad \text{(A-5)}
$$

relative to the lower left-hand corner of the element waveguide. A time dependence of $\exp(j\omega t)$ is understood, and

$$
\gamma_{pq} = k_o\sqrt{\left[\frac{p\lambda}{2a}\right]^2 + \left[\frac{q\lambda}{2b}\right]^2 - \epsilon_r} \qquad \text{(A-6)}
$$

where ϵ_r is the relative dielectric constant in the waveguide.

It is assumed that energy is incident from inside the element waveguides with an amplitude of unity and in the dominant TE mode having $p = 1$ and $q = 0$, and so the wave has its "principal" polarization in the y-direction. It is further assumed that the wave is reflected from the plane of the surface of the array with a voltage reflection coefficient R. The total transverse field can now be written for the entire cross section represented by the array space cell. It is assumed that the outline of the free space cell extends in both directions from the face of the array.

At a point $z \leq 0$ the transverse fields for the triangular grid are written according to the following auziliary definitions.

$$U_1 = 1; \quad -\frac{a}{2} \leq x \leq \frac{a}{2}, \quad -\frac{b}{2} \leq y \leq \frac{b}{2}$$

$$= 0; \quad \text{elsewhere}$$

$$U_2 = I; \quad -\frac{A}{2} \leq x \leq -\frac{A}{2} + \frac{a}{2}, \quad \frac{B}{2} - \frac{b}{2} \leq y \leq \frac{B}{2}$$

$$= 0; \quad \text{elsewhere}$$

$$U_3 = I; \quad -\frac{A}{2} \leq x \leq -\frac{A}{2} + \frac{a}{2}, \quad -\frac{B}{2} \leq y \leq -\frac{B}{2} + \frac{b}{2}$$

$$= 0; \quad \text{elsewhere}$$

$$U_4 = I; \quad \frac{A}{2} - \frac{a}{2} \leq x \leq \frac{A}{2}, \quad \frac{B}{2} - \frac{b}{2} \leq y \leq \frac{B}{2}$$

$$= 0; \quad \text{elsewhere}$$

$$U_5 = I; \quad \frac{A}{2} - \frac{a}{2} \leq x \leq \frac{A}{2}, \quad -\frac{B}{2} \leq y \leq -\frac{B}{2} + \frac{b}{2}$$

$$= 0; \quad \text{elsewhere}$$

$$u_{x1} = 0, \qquad u_{y1} = 0$$

$$u_{x2} = -\frac{A}{2}, \quad u_{y2} = \frac{B}{2}$$

$$u_{x3} = -\frac{A}{2}, \quad u_{y3} = -\frac{B}{2}$$

$$u_{x4} = \frac{A}{2}, \quad u_{y4} = \frac{B}{2}$$

$$u_{x5} = \frac{A}{2}, \quad u_{y5} = -\frac{B}{2}$$

where "I" is unity for uniform amplitude elements in a triangular grid. Note that the unit cell dimensions are such that if I = 0, the above definitions also describe the rectangular grid. Within a unit cell, at a point $z \leq 0$ below the face of the array the transverse fields are

$$E_x = -\sum_{p=0}^{\infty} \sum_{q=1}^{\infty} \left[E_{pq} \frac{q\pi}{b} - H_{pq} \frac{p\pi}{a} \right] \sum_{i=1}^{5} U_i \cos \frac{p\pi \left[x + \frac{a}{2} - u_{xi} \right]}{a} \tag{A-7}$$

$$\sin \frac{q\pi \left[y + \frac{b}{2} - u_{yi} \right]}{b} e^{-j k_x u_{xi}} e^{-j k_y u_{yi}} e^{\gamma_{pq} z}$$

$$E_y = \left[e^{-\gamma_{10} z} + \mathrm{Re}^{\gamma_{10} z}\right] \frac{\pi}{a} \sum_{i=1}^{5} U_i \sin \frac{\pi\left[x + \frac{a}{2} - u_{xi}\right]}{a} e^{-j k_x u_{xi}} e^{-j k_y u_{yi}}$$

$$+ \sum_{p=1}^{\infty} \sum_{q=0}^{\infty}{}' \left[E_{pq} \frac{p\pi}{a} + H_{pq} \frac{q\pi}{b}\right] \sum_{i=1}^{5} U_i \sin \frac{p\pi\left[x + \frac{a}{2} - u_{xi}\right]}{a}$$

$$\cos \frac{q\pi\left[y + \frac{b}{2} - u_{yi}\right]}{b} e^{-j k_x u_{xi}} e^{-j k_y u_{yi}} e^{\gamma_{pq} z}$$

$$H_x = -\left[e^{-\gamma_{10} z} - \mathrm{Re}^{\gamma_{10} z}\right] \frac{\pi}{a} \frac{\gamma_{10}}{j\omega\mu} \sum_{i=1}^{5} U_i \sin \frac{\pi\left[x + \frac{a}{2} - u_{xi}\right]}{a} e^{-j k_x u_{xi}} e^{-j k_y u_{yi}}$$

$$+ \sum_{p=1}^{\infty} \sum_{q=0}^{\infty}{}' \left[E_{pq} \frac{p\pi}{a} \frac{\gamma_{pq}}{j\omega\mu} + H_{pq} \frac{q\pi}{b} \frac{j\omega\epsilon_r}{\gamma_{pq}}\right] \sum_{i=1}^{5} U_i \sin \frac{p\pi\left[x + \frac{a}{2} - u_{xi}\right]}{a} \qquad \text{(A-7)}$$

$$\cos \frac{q\pi\left[y + \frac{b}{2} - u_{yi}\right]}{b} e^{-j k_x u_{xi}} e^{-j k_y u_{yi}} e^{\gamma_{pq} z}$$

$$H_y = \sum_{p=0}^{\infty} \sum_{q=1}^{\infty} \left[E_{pq} \frac{q\pi}{b} \frac{\gamma_{pq}}{j\omega\mu} - H_{pq} \frac{p\pi}{a} \frac{j\omega\epsilon_r}{\gamma_{pq}}\right] \sum_{i=1}^{5} U_i \cos \frac{p\pi\left[x + \frac{a}{2} - u_{xi}\right]}{a}$$

$$\sin \frac{q\pi\left[y + \frac{b}{2} - u_{yi}\right]}{b} e^{-j k_x u_{xi}} e^{-j k_y u_{yi}} e^{\gamma_{pq} z}$$

where $\sum_{p=1}^{\infty} \sum_{q=0}^{\infty}{}'$ signifies that the mode p=1, q=0 is to be excluded from the summation.

The summations with "i" as the index accommodate the partial waveguide apertures at the four corners of the unit cell in their proper phases relative to the waveguide at the center of the cell by virtue of the definitions given above.

Within a unit cell, at a point $z \geq 0$ in the free space region above the face of the array, the transverse fields are

$$E_x = -\sum_{-\infty}^{\infty} \sum_{-\infty}^{\infty} \left[V_{mn} \beta_n - M_{mn} \beta_m\right] e^{-j \beta_m x} e^{-j \beta_n y} e^{-\Gamma_{mn} z} \qquad \text{(A-8)}$$

$$E_y = \sum_{-\infty}^{\infty}\sum_{-\infty}^{\infty}\left[V_{mn}\,\beta_m + M_{mn}\,\beta_n\right] e^{-j\,\beta_m x}\, e^{-j\,\beta_n y}\, e^{-\Gamma_{mn} z}$$

$$H_x = -\sum_{-\infty}^{\infty}\sum_{-\infty}^{\infty}\left[V_{mn}\,\beta_m\,\frac{\Gamma_{mn}}{j\omega\mu} + M_{mn}\,\beta_n\,\frac{j\omega\epsilon}{\Gamma_{mn}}\right] e^{-j\,\beta_m x}\, e^{-j\,\beta_n y}\, e^{-\Gamma_{mn} z} \qquad \text{(A-8)}$$

$$H_y = -\sum_{-\infty}^{\infty}\sum_{-\infty}^{\infty}\left[V_{mn}\,\beta_n\,\frac{\Gamma_{mn}}{j\omega\mu} - M_{mn}\,\beta_m\,\frac{j\omega\epsilon}{\Gamma_{mn}}\right] e^{-j\,\beta_m x}\, e^{-j\,\beta_n y}\, e^{-\Gamma_{mn} z}$$

In Equations (A-7) and (A-8), the longitudinal fields E_z and H_z have been omitted from consideration because they are derivable from the transverse fields through Maxwell's equations and therefore presenting them would be redundant.

At this point we have expressions for the components of the total possible field that may exist on each side of the plane of the face of the array. In the plane of the junction ($z = 0$) the field in the waveguide system must equal and be continuous with the field in the free space region over the cross section of the unit cell. Therefore,

$$\begin{aligned} E_x\,(\text{waveguide})\,\Big|_{z=0} &= E_x\,(\text{free space})\,\Big|_{z=0} \\ E_y\,(\text{waveguide})\,\Big|_{z=0} &= E_y\,(\text{free space})\,\Big|_{z=0} \end{aligned} \qquad \text{(A-9)}$$

with a range of validity that extends over the entire cross section of the cell since, at points other than within a waveguide aperture, the electric field is parallel with a conducting surface and is therefore identically zero. A magnetic field parallel with a conducting surface is discontinuous at the surface by an amount of the surface current so the magnetic field continuity equations

$$\begin{aligned} H_x\,(\text{waveguide})\,\Big|_{z=0} &= H_x\,(\text{free space})\,\Big|_{z=0} \\ H_y\,(\text{waveguide})\,\Big|_{z=0} &= H_y\,(\text{free space})\,\Big|_{z=0} \end{aligned} \qquad \text{(A-10)}$$

are valid only over the cross sections of the waveguide apertures (or fractional apertures) within the boundaries of the cell.

Since the electric field continuity equations are valid everywhere, let us multiply both sides of each equation by the function

$$e^{j\beta_r x} \; e^{j\beta_s y}$$

orthogonal to the free space set, and integrate over the cell cross section. The result of the integration on the free space side of the equations is zero except when r = m and s = n, from which we obtain expressions for

$$V_{mn}\,\beta_n - M_{mn}\,\beta_m$$

and

$$V_{mn}\,\beta_m + M_{mn}\,\beta_n$$

from the E_x and E_y continuity equations, respectively. These are readily solved for V_{mn} and M_{mn}, but first let us define the following functions.

$$S_m(p) = \frac{\sin\left[\frac{\beta_m a}{2} - \frac{p\pi}{2}\right]}{\left[\frac{\beta_m a}{2}\right]^2 - \left[\frac{p\pi}{2}\right]^2}$$

$$S_n(q) = \frac{\sin\left[\frac{\beta_n b}{2} - \frac{q\pi}{2}\right]}{\left[\frac{\beta_n b}{2}\right]^2 - \left[\frac{q\pi}{2}\right]^2} \qquad \text{(A-11)}$$

$$\delta_{mn} = 1 + I \cos m\pi \cos n\pi$$

where as before "I" is unity for a triangular grid and zero for a rectangular grid. As a result

$$V_{mn} = j\,\frac{ab}{AB}\,\delta_{mn}\left[(1+R)\left[\frac{\pi}{2}\right]^2 \frac{b}{a}\,\frac{\beta_m\,\beta_n}{\beta_m^{\,2}+\beta_n^{\,2}}\,S_m(1)\,S_n(0)\,e^{-j\frac{\pi}{2}}\right.$$

$$+\frac{a}{2}\,\frac{\beta_m\,\beta_n}{\beta_m^{\,2}+\beta_n^{\,2}}\sum_{p=0}^{\infty}\sum_{q=1}^{\infty}\left[E_{pq}\,\frac{q\pi}{b} - H_{pq}\,\frac{p\pi}{a}\right]\frac{q\pi}{2}\cdot S_m(p)\,S_n(q)\,e^{-j\frac{p\pi}{2}}\,e^{-j\frac{q\pi}{2}} \qquad \text{(A-12)}$$

$$\left.+\frac{b}{2}\,\frac{\beta_m\,\beta_n}{\beta_m^{\,2}+\beta_n^{\,2}}\sum_{p=1}^{\infty}\sum_{q=0}^{\infty}{}'\left[E_{pq}\,\frac{p\pi}{a} + H_{pq}\,\frac{q\pi}{b}\right]\frac{p\pi}{2}\cdot S_m(p)\,S_n(q)\,e^{-j\frac{p\pi}{2}}\,e^{-j\frac{q\pi}{2}}\right]$$

$$M_{mn} = j \frac{ab}{AB} \delta_{mn} \left[(1 + R) \left[\frac{\pi}{2}\right]^2 \frac{b}{a} \frac{\beta_n^2}{\beta_m^2 + \beta_n^2} S_m(1)\, S_n(0)\, e^{-j\frac{\pi}{2}} \right. \tag{A-13}$$

$$- \frac{a}{2} \frac{\beta_m^2}{\beta_m^2 + \beta_n^2} \sum_{p=0}^{\infty} \sum_{q=1}^{\infty} \left[E_{pq} \frac{q\pi}{b} - H_{pq} \frac{p\pi}{a} \right] \frac{q\pi}{2} \cdot S_m(p)\, S_n(q)\, e^{-j\frac{p\pi}{2}} e^{-j\frac{q\pi}{2}}$$

$$\left. + \frac{b}{2} \frac{\beta_n^2}{\beta_m^2 + \beta_n^2} \sum_{p=1}^{\infty} \sum_{q=0}^{\infty}{}' \left[E_{pq} \frac{p\pi}{a} + H_{pq} \frac{q\pi}{b} \right] \frac{p\pi}{2} \cdot S_m(p)\, S_n(q)\, e^{-j\frac{p\pi}{2}} e^{-j\frac{q\pi}{2}} \right]$$

It has been pointed out that the magnetic field continuity equations are valid only with the confines of the waveguide apertures (or partial apertures) enclosed by the cell. Therefore, let us multiply both sides of each equation by the appropriate function for each that is orthogonal to the waveguide set, and integrate over the enclosed waveguide apertures. For H_x, the appropriate function is

$$\sum_{i=1}^{5} U_i \sin \frac{r\pi(x + \frac{a}{2} - u_{xi})}{a} \cos \frac{s\pi(y + \frac{b}{2} - u_{yi})}{b} e^{j k_x u_{xi}} e^{j k_y u_{yi}}$$

and for H_y, it is

$$\sum_{i=1}^{5} U_i \cos \frac{r\pi(x + \frac{a}{2} - u_{xi})}{a} \sin \frac{s\pi(y + \frac{b}{2} - u_{yi})}{b} e^{j k_x u_{xi}} e^{j k_y u_{yi}}$$

Before performing the integration let us replace p and q by P and Q, respectively, in order to avoid confusion later on in the development. The results of the integration on the waveguide side of the equations is zero except when r = P and s = Q. From the H_x continuity equation we obtain

$$1 - R = \frac{j\omega\mu}{\gamma_{10}} a \sum_{-\infty}^{\infty} \sum_{-\infty}^{\infty} \frac{\delta_{mn}}{1+I} \left[V_{mn} \beta_m \frac{\Gamma_{mn}}{j\omega\mu} + M_{mn} \beta_n \frac{j\omega\epsilon_o}{\Gamma_{mn}} \right] \frac{\beta_n b}{2} S_m(1)\, S_n(0) \tag{A-14}$$

and

$$E_{PQ}\,\frac{P\pi}{a}\,\frac{\gamma_{PQ}}{j\omega\mu} + H_{PQ}\,\frac{Q\pi}{b}\,\frac{j\omega\epsilon_r}{\gamma_{PQ}}$$

$$= j2\epsilon_{OQ}\,\frac{P\pi}{2}\sum_{-\infty}^{\infty}\sum_{-\infty}^{\infty}\frac{\delta_{mn}}{1+I}\left[V_{mn}\,\beta_m\,\frac{\Gamma_{mn}}{j\omega\mu} + M_{mn}\,\beta_n\,\frac{j\omega\epsilon_o}{\Gamma_{mn}}\right]\frac{\beta_n b}{2} \qquad \text{(A-15)}$$

$$\cdot\; S_m(P)\,S_n(Q)\,e^{j\frac{P\pi}{2}}\,e^{j\frac{Q\pi}{2}}$$

where

$$\epsilon_{OQ} = 1 \quad \text{if } Q = 0$$

$$= 2 \quad \text{otherwise}$$

From the H_y continuity equation we get

$$E_{PQ}\,\frac{Q\pi}{b}\,\frac{\gamma_{PQ}}{j\omega\mu} - H_{PQ}\,\frac{P\pi}{a}\,\frac{j\omega\epsilon_r}{\gamma_{PQ}}$$

$$= j2\epsilon_{OP}\,\frac{Q\pi}{2}\sum_{-\infty}^{\infty}\sum_{-\infty}^{\infty}\frac{\delta_{mn}}{1+I}\left[V_{mn}\,\beta_n\,\frac{\Gamma_{mn}}{j\omega\mu} - M_{mn}\,\beta_m\,\frac{j\omega\epsilon_o}{\Gamma_{mn}}\right]\frac{\beta_m a}{2} \qquad \text{(A-16)}$$

$$\cdot\; S_m(P)\,S_n(Q)\,e^{j\frac{P\pi}{2}}\,e^{j\frac{Q\pi}{2}}$$

where

$$\epsilon_{OP} = 1 \quad \text{if } P = 0$$

$$= 2 \quad \text{otherwise}$$

Let us now consider the substitution of V_{mn} and M_{mn} from Equations (A-12) and (A-13) into Equations (A-14), (A-15), and (A-16). After having done so, we can define a new pair of amplitude coefficients.

$$C_{pq} = \frac{a}{\pi}\,\frac{1}{1+R}\left[E_{pq}\,\frac{q\pi}{b} - H_{pq}\,\frac{p\pi}{a}\right]e^{-j\frac{p\pi}{2}}\,e^{-j\frac{q\pi}{2}} \qquad \text{(A-17)}$$

$$D_{pq} = \frac{a}{\pi}\,\frac{1}{1+R}\left[E_{pq}\,\frac{p\pi}{a} + H_{pq}\,\frac{q\pi}{b}\right]e^{-j\frac{p\pi}{2}}\,e^{-j\frac{q\pi}{2}} \qquad \text{(A-18)}$$

UNCLASSIFIED

Security Classification

DOCUMENT CONTROL DATA – R&D

(Security classification of title, body of abstract and indexing annotation must be entered when the overall report is classified)

1. ORIGINATING ACTIVITY *(Corporate author)*
General Electric Company under P.O. No. C-487

2a. REPORT SECURITY CLASSIFICATION
Unclassified

2b. GROUP
None

3. REPORT TITLE
Mutual Coupling Study

4. DESCRIPTIVE NOTES *(Type of report and inclusive dates)*
Technical Report

5. AUTHOR(S) *(Last name, first name, initial)*
Farrell, George F., Jr.

6. REPORT DATE	7a. TOTAL NO. OF PAGES	7b. NO. OF REFS
31 March 1967	64	3

8a. CONTRACT OR GRANT NO.
AF 19(628)-5167

b. PROJECT NO.
ARPA Order 498

c.

d.

9a. ORIGINATOR'S REPORT NUMBER(S)
GE Purchase Order No. EH-40039

9b. OTHER REPORT NO(S) *(Any other numbers that may be assigned this report)*
ESD-TR-67-279

10. AVAILABILITY/LIMITATION NOTICES
Distribution of this document is unlimited.

11. SUPPLEMENTARY NOTES
None

12. SPONSORING MILITARY ACTIVITY
Advanced Research Projects Agency, Department of Defense

13. ABSTRACT

This report gives the complete derivation (in an appendix) of the radiation admittance of a rectangular waveguide acting as an element in an infinite phased array. The derived equations are capable of predicting the experimentally observed anomalous notch that has been found to exist in arrays composed of large waveguides. The defining equations demonstrate that it is the existence of nonpropagating higher order modes inside the element waveguides that determine the behavior of an infinite array.

It was the purpose of this study to determine what waveguide modes were important for a reasonably confident prediction of the radiation admittance of a rectangular waveguide in an array. It is shown that the number of modes needed for this is not excessively great, but that more are needed if it is desired to predict the position of an anomalous notch with any great degree of confidence.

14. KEY WORDS

phased arrays
waveguide couplers
rectangular waveguide

UNCLASSIFIED

Security Classification

GENERAL ELECTRIC